Supporting Information to accompany:

Surface Barriers of Hydrocarbon Transport Triggered by Ideal Zeolite Structures

Nils E. R. Zimmermann,[*,†] Sayee P. Balaji,[†,‡] and Frerich J. Keil[†]

Chemical Reaction Engineering, Hamburg University of Technology, Eissendorfer Str. 38, 21073 Hamburg, Germany

E-mail: nils.zimmermann@tu-harburg.de

[*]To whom correspondence should be addressed

[†]Hamburg University of Technology

[‡]Current address: Process & Energy Laboratory, Delft University of Technology, Leeghwaterstraat 44, 2628 CA Delft, The Netherlands

Contents

1 Methodology Details

1.1 Molecular Simulations

The main results of the molecular simulations were equilibrium fluxes between adjacent adsorption sites which were identified by free-energy profiles (see also Figure 1 of the main text). Two fluxes were computed for each system. The first one characterized the equilibrium rate of transport between internal sites, i.e. in the "periodic" zeolite ($j^{\ddagger}_{\text{zeol}}$). The second flux was calculated at the external surface ($j^{\ddagger}_{\text{surf}}$); to be more precise, the transport between the outermost cage of the zeolite slab and the external surface was being determined. As in our previous work,[1] the concepts of dynamically corrected transition state theory were applied for computing transport rates, mainly implying a two step procedure to flux calculation:

1. concentration at dividing surface, $c(q^{\ddagger})$, and

2. transmission coefficient, κ.

Concentration profiles were obtained from residence histograms, $P(q)$, sampled in NVT Monte Carlo (MC) simulations. Trial moves included displacements, rotations and regrow (partial and full) of the molecules. Instead of the center of mass position of an entire molecule, the position of that bead which was located closest to the center of the CH_x chain had been defined as reaction coordinate (reactive bead):

- methane, ethane and ethene $\rightarrow$ bead 1;

- propane, propene, and butane $\rightarrow$ bead 2;

- pentane and hexane $\rightarrow$ bead 3.

In order to determine the concentration profiles and thus the concentrations at the dividing surfaces of interest, the computed residence-probability profiles were scaled to match the units and magnitude of the bulk gas concentration because $P(q) \propto c(q)$ and hence $P_{\text{gas}} \propto c_{\text{gas}}$. Assuming the

mean velocity of the molecules obey the kinetic theory of gases yields the ideal transition state theory flux, $j^{\ddagger}_{\mathrm{TST}}$:

$$j^{\ddagger}_{\mathrm{TST}} = c(q^{\ddagger}) \cdot \sqrt{\frac{k_{\mathrm{B}}T}{2\pi m_{\mathrm{fluid}}}}, \tag{1}$$

where ‡ indicates the position of the dividing surface (free-energy maximum) and m_{fluid} is the mass of the bead involved in the residence-histogram determination. Note that the square root term in Eq. (1) cancels out exactly for the computation of the critical membrane thickness because it is proportional to the ratio of the fluxes (same m_{fluid} and at the same T).

The transmission coefficients (κ) were determined by means of reactive flux (RF) simulations for which the reactive bead of the tagged molecule was, in the starting configuration, constrained to the dividing surface. The molecular dynamics part of the RF simulations was performed in the NVE ensemble and the transmission coefficient was identified as the plateau value of the transient reactive flux correlation function [$\kappa = \lim_{t\to\infty} \kappa(t)$].[2] The dynamically corrected flux follows:

$$j^{\ddagger}_{\mathrm{dcTST}} = \kappa \cdot j^{\ddagger}_{\mathrm{TST}} = \kappa \cdot c(q^{\ddagger}) \cdot \sqrt{\frac{k_{\mathrm{B}}T}{2\pi m_{\mathrm{fluid}}}}. \tag{2}$$

As in our previous study,[1] the bulk fluid concentration and the core zeolite loading were sampled. The agreement of the thus determined isotherms is excellent with data from Grand-Canonical (GC) MC simulations, see Figure S1.

Except for the zero-pressure/zero-loading limit where a single fluid molecule was put into the entire simulation box, the finite-pressure simulations were performed with 10, 20, 50 and 100 molecules, respectively. The pressure was calculated on the basis of the mean bulk gas concentration and the Peng-Robinson equation of state.

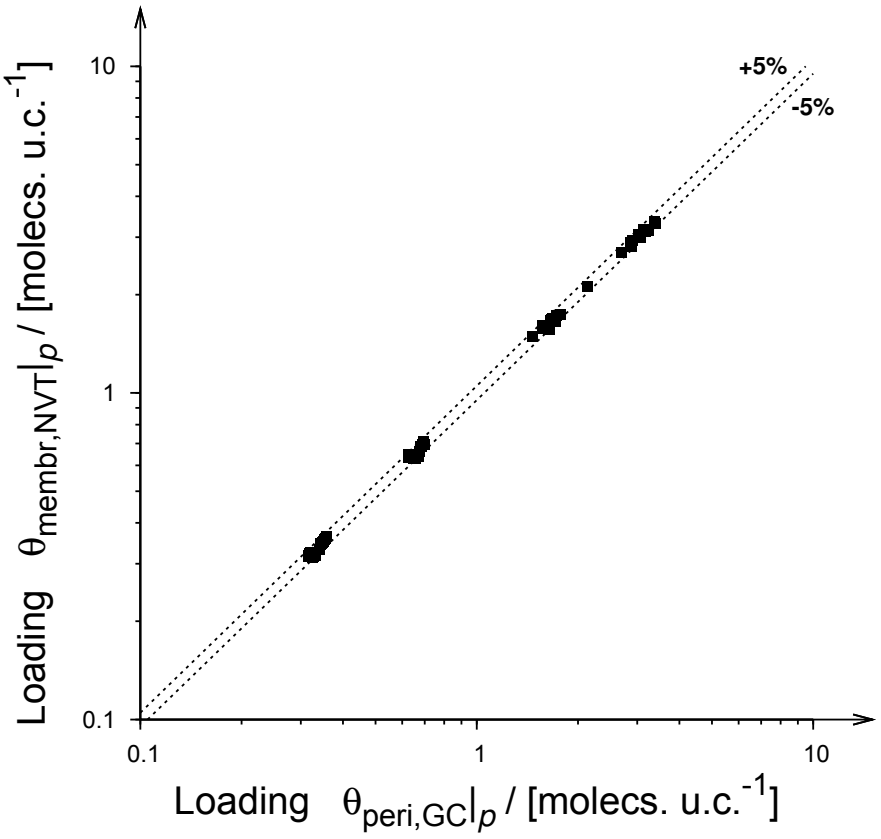

Figure S1: Parity plot; loading from NVT-MC simulations using a single-crystal zeolite membrane, $\theta_{membr,NVT}$, *vs*. loading from conventional GCMC simulations in a fully periodic zeolite , $\theta_{peri,GC}$, at equal gas pressure, p. Results are from all guest-host systems studied. The lines indicate the region of $\pm 5\%$ deviation.

1.2 Force Field Parameters

The intramolecular interactions of the *n*-alkanes and *n*-alkenes consisted of bond stretching (harmonic potential), bond-angle bending (harmonic cosine potential), and torsion (cosine power series of the dihedral angle), see Table S1.

TABLE S1: Bond stretching, bond-angle bending, and torsion parameters.[a]

Potential	Bond Pattern	k_i/k_B	r_{eq}
		η_i/k_B	ϕ_{eq}
			i
$U_{bond} = 1/2\ k_{bond}\ (r - r_{eq})^2$	$CH_3(sp^3) - CH_3(sp^3)$	96,500 K/Å^2	1.54 Å
	$CH_3(sp^3) - CH_2(sp^3)$		
	$CH_2(sp^3) - CH_2(sp^3)$		
	$CH_2(sp^2) = CH_2(sp^2)$	786,873 K/Å^2	1.33 Å
	$CH_2(sp^2) = CH(sp^2)$	785,050 K/Å^2	1.33 Å
	$CH(sp^2) - CH_3(sp^3)$	251,549 K/Å^2	1.54 Å
$U_{bend} =$	$CH_3(sp^3) - CH_2(sp^3) - CH_3(sp^3)$	62,500 K	114.0°
$1/2\ k_{bend}\ (\cos\phi - \cos\phi_{eq})^2$	$CH_3(sp^3) - CH_2(sp^3) - CH_2(sp^3)$		
	$CH_2(sp^3) - CH_2(sp^3) - CH_2(sp^3)$		
$U_{bend} = 1/2\ k_{bend}\ (\phi - \phi_{eq})^2$	$CH_2(sp^2) - CH(sp^2) - CH_3(sp^3)$	70,400 K/rad^2	119.7°
$U_{torsion} = \sum_{i=0}^{5} \eta_i\ \cos^i\phi$	$R_1 - CH_2(sp^3) - CH_2(sp^3) - R_2$	1,204.654 K	0
		1,947.740 K	1
		-357.845 K	2
		-1,944.666 K	3
		715.690 K	4
		-1,565.572 K	5

[a] *R_1 and R_2 represent any possible alkyl remainder, i.e. $CH_3(sp^3)$ or $CH_3(sp^3) - CH_2(sp^3)$.*

In Table S2, the Lennard-Jones force field parameters used in this work are listed. The parameters in bold italics highlight those values that differ slightly from the original ones proposed by Dubbeldam et al.[3] and Liu et al.[4] The impact of the resulting force field differences is entirely negligible for our results, see also discussion below. Viewed from a different perspective, we can therefore state that our *main conclusions*, i.e. that the three most important variables to surface barriers have been identified as thermodynamic state of bulk fluid, nanopore smoothness, and host material density, are *insensitive against the force field* chosen.

TABLE S2: Lennard-Jones parameters.[a]

Atom/bead			CH_4	$CH_3(sp^3)$	$CH_2(sp^3)$	$CH_2(sp^2)$	$CH(sp^2)$
CH_4	ε_{ij}/k_B	[K]	158.50				
	σ_{ij}	[Å]	3.72				
$CH_3(sp^3)$	ε_{ij}/k_B	[K]		108.00	77.77		
	σ_{ij}	[Å]		3.76	3.86		
$CH_2(sp^3)$	ε_{ij}/k_B	[K]		77.77	***77.77***		
	σ_{ij}	[Å]		3.86	***3.86***		
$CH_2(sp^2)$	ε_{ij}/k_B	[K]				***85.000***	***63.206***
	σ_{ij}	[Å]				***3.675***	***3.703***
$CH(sp^2)$	ε_{ij}/k_B	[K]				***63.206***	53.000
	σ_{ij}	[Å]				***3.703***	3.740
O (zeolite)	ε_{iO}/k_B	[K]	115.00	93.00	60.50	82.050	55.215
	σ_{iO}	[Å]	3.47	3.48	3.58	3.530	3.502

[a] *Parameters in bold italics indicate differences to original ones from Refs. 3 and 4.*

The original Lennard-Jones parameters from Refs. 3 and 4 and the resulting relative difference [i.e. $\Delta\sigma = (\sigma - \sigma_{\text{original}})/\sigma_{\text{original}}$] are:

- **$CH_2(sp^3)$–$CH_2(sp^3)$**: σ =3.96 Å ($\Delta\sigma$ =–2.5%), ε/k_B =56.0 K ($\Delta\varepsilon$ =+38.9%);
- **$CH_2(sp^2)$–$CH_2(sp^2)$**: σ =3.685 Å ($\Delta\sigma$ =–0.3%), ε/k_B =93.0 K ($\Delta\varepsilon$ =–8.6%);

- **$CH_2(sp^2)$–$CH(sp^2)$**: σ =3.71 Å ($\Delta\sigma$ =–0.2%), ε/k_B =70.21 K ($\Delta\varepsilon$ =–10.0%).

From this list follows that the results of ethene, propene, propane, butane, pentane, and hexane were affected, and that the relative difference in the guest-guest Lennard-Jones parameters varied between –10% and +39%. We, however, need to stress at this point that this concerned the *finite loading* results only. The simulation results with only one molecule in the box, i.e. where the strongest surface-barrier effects have been observed, were not affected *at all*.

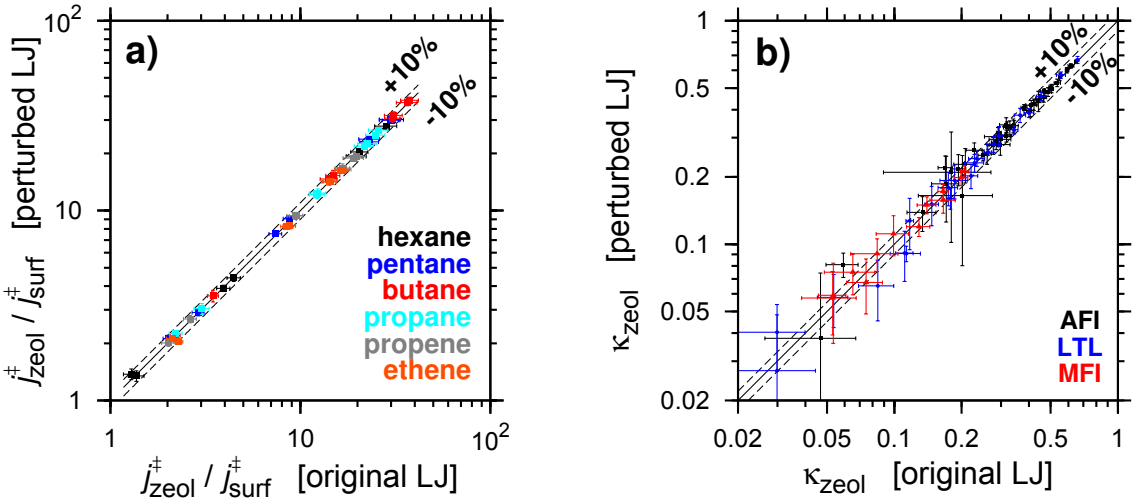

Figure S2: Parity plots: a) flux ratio, $j^{\ddagger}_{zeol}/j^{\ddagger}_{surf} \propto \delta_{crit}$, of all molecules affected by the parameter perturbation in AFI; b) transmission coefficients in periodic structure, κ_{zeol}, of all affected molecules in all three zeolites studied.

To assess whether or not the partly large differences in Lennard-Jones parameters imply similarly strong deviations in the results, roughly one third of the simulations were rerun with the correct parameters. In particular, all affected AFI-histogram simulations were repeated, as well as all affected transmission coefficient simulations in all three periodic zeolite structures (κ_{zeol}). The correspondence between the results obtained with original and slightly perturbed parameters are displayed in Figure S2. Since the central results of this work are critical membrane thicknesses which scale with the ratio of the fluxes involved (i.e. $j^{\ddagger}_{zeol}/j^{\ddagger}_{surf}$) the ratios rather than the fluxes themselves are plotted in Figure S2a. As can be seen from the figure, the vast majority of the results

from the two parameter sets agree very well with each other. In the few cases when the deviation is larger than $\pm 10\%$ (dashed lines), the error bars are usually so large that the uncertainty area of a given data point finally overlaps again with the 10%-agreement region.

The absence of any considerable systematic deviation can be explained by the domination of the zeolite force field over the interaction that guest molecules exert on one another. The Lennard-Jones parameters of a given CH_x bead to interact with another bead of the same kind (CH_x – CH_x) is similar to the interaction parameters with the zeolite oxygen (CH_x – O). There are usually only few other beads of the same kind which surround this CH_x bead because of the rather low loadings establishing in our simulations. However, the situation is entirely different in regard to the zeolite O-atoms which surround the CH_x under consideration by hundreds. Hence, the guest-host interaction vastly dominates over any other contribution to the potential, and the results do thus not show any significant sensitivity towards small to moderate deviations in the (guest–guest) force field parameters which is understandable and finally justifies the use of the force field employed.

1.3 Tracer-Exchange Curves

The single-crystal membrane was modeled as a plate of infinite cross section (x-y) and of thickness δ in z direction. Furthermore, it was divided into n_s slabs, each of width Δz, see also Figure S3; hence $n_s \times \Delta z = \delta$ and the center was located at $z = 0$. Depending on the zeolite, the slab width represents either the separation between adjacent cages (AFI, LTL) or the intersection separation (MFI), i.e. $\Delta z = \lambda$.

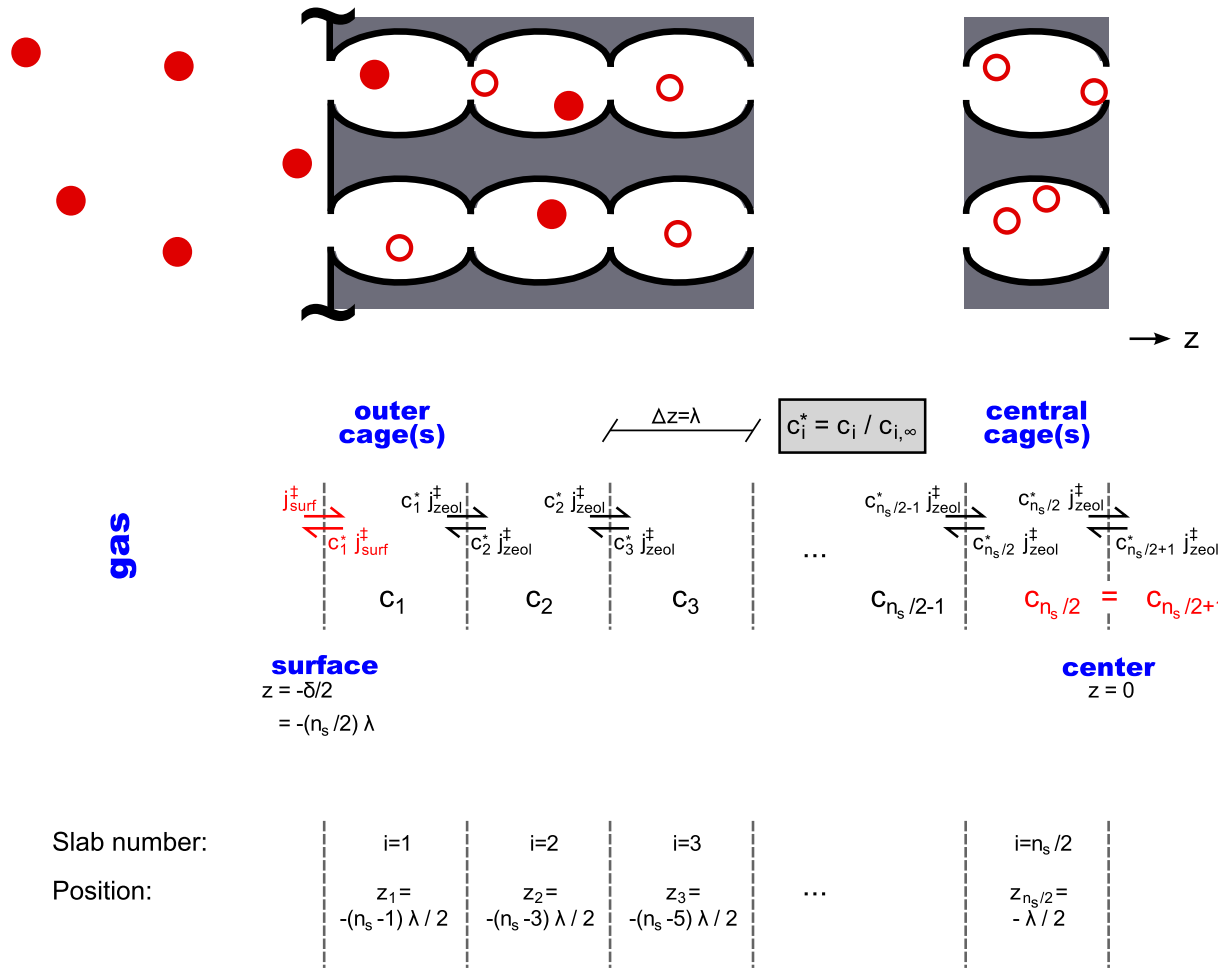

Figure S3: Scheme of spatial set-up of the tracer-exchange continuum simulations. Note that $c_i^* = c_i / c_{i,\infty}$.

The first step of the tracer-exchange curve computation was the determination of successive concentration profiles, $c(t,z) = c_{\text{labeled}}(t,z)$.* This was accomplished by numerical integration of Fick's second law of the initially empty membrane: $c(0,z) = 0$. The fluxes $j^{\ddagger}_{\text{zeol}}$ and $j^{\ddagger}_{\text{surf}}$ from the molecular simulations served as input to the continuum simulations.

The incremental change in concentration for slab number i follows (finite difference formula):

$$\begin{aligned}
\Delta c_i(t+\Delta t) &= \frac{j^{\ddagger}_{\text{zeol}}[c_{i-1}(t)/c_{i-1,\infty} - 2c_i(t)/c_{i,\infty} + c_{i+1}(t)/c_{i+1,\infty}]}{\Delta z} \cdot \Delta t, && (3)\\
&= \frac{j^{\ddagger}_{\text{zeol}}[c^*_{i-1}(t) - 2c^*_i(t) + c^*_{i+1}(t)]}{\Delta z} \cdot \Delta t, && (4)\\
&= \frac{j^{\ddagger}_{\text{zeol}}[c_{i-1}(t) - 2c_i(t) + c_{i+1}(t)]}{\langle c_{\text{zeol}}\rangle \cdot \Delta z} \cdot \Delta t, && (5)
\end{aligned}$$

with $c_i = c(z_i)$, $j^{\ddagger}_{\text{zeol}}$ the flux between adjacent cages/intersections, $\langle c_{\text{zeol}}\rangle$ the equilibrium concentration which is obtained from the isotherm converting the loading θ into a concentration in [mol m^{-3}], and Δt is the time increment. In Eq. 4, all $c_{i,\infty}$ were assumed to be equal ($c_{i,\infty} = \langle c_{\text{zeol}}\rangle$). This is justified because the proximity to the surface induces a slightly different potential-energy field to the very first slab only. As can be seen from the free-energy plot in Figure 1 of the main text, this perturbation vanishes yet already for the second slab.

Symmetry conditions were applied in the membrane center (right-hand side in Figure S3):

$$\Delta c_{n_s/2}(t+\Delta t) = \frac{j^{\ddagger}_{\text{zeol}}[c_{n_s/2-1}(t) - c_{n_s/2}(t)]}{\langle c_{\text{zeol}}\rangle \cdot \Delta z} \cdot \Delta t, \qquad (6)$$

At the membrane entrance (left-hand side in Figure S3), the surface flux constituted the boundary condition:

$$\Delta c_1(t+\Delta t) = \frac{j^{\ddagger}_{\text{surf}}[1 - c_1(t)/c_{\text{surf},\infty}] + j^{\ddagger}_{\text{zeol}}[c_2(t)/\langle c_{\text{zeol}}\rangle - c_1(t)/c_{\text{surf},\infty}]}{\Delta z} \cdot \Delta t, \qquad (7)$$

where $j^{\ddagger}_{\text{surf}}$ denotes the flux prevailing at the surface and $c_{\text{surf},\infty}$ is the equilibrium concentration in

*Note that $c_{\text{total}}(z) = c_{\text{labeled}}(t,z) + c_{\text{unlabeled}}(t,z)$ is constant at all times for a given slab because of the condition of tracer exchange.

the very first slab.

After having determined a given concentration profile at time t, the mass exchanged at that time, $M(t)$, could be computed because of its proportionality to the concentration integral along z:

$$M(t) \propto \int_{-\delta/2}^{+\delta/2} c(t,z)\,\mathrm{d}z. \tag{8}$$

The curve was normalized with the integral after long time $t \to \infty$ (i.e. with the adsorption capacity) to finally yield the fractional exchange amount:

$$\frac{M(t)}{M_\infty} = \frac{\int_{-\delta/2}^{+\delta/2} c(t,z)\,\mathrm{d}z}{\lim_{t\to\infty} \int_{-\delta/2}^{+\delta/2} c(t,z)\,\mathrm{d}z}. \tag{9}$$

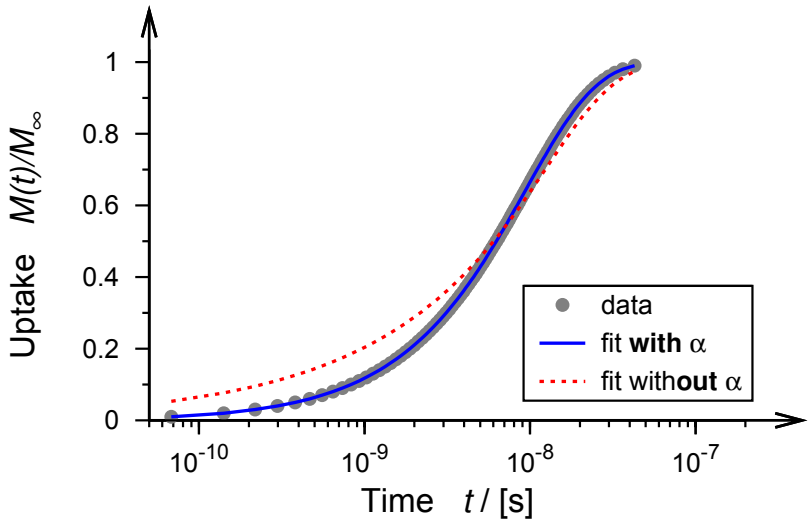

Figure S4: Fractional amount of tracer exchanged, $M(t)/M_\infty$, for propane in an AFI membrane (T =388 K, P =53594 Pa, δ = 25.452 nm).

As an example, Figure S4 depicts a tracer-exchange curve of a membrane which was initially filled with unlabeled molecules (empty $\rightarrow$ tracer adsorption. The input fluxes came from a propane

simulation in an AFI membrane. Along with the data, fitted curves are presented using the two different approaches described in the main text.

1.4 Effective Self-Diffusion Coefficient

In Figure S5, four examples of the increase of $D_{S,eff}$ with membrane thickness are presented. The critical value gives a good estimate of that membrane thickness where the deviation between the true diffusivity and the effective one is still large (factors of 3.6...4.5). So, it helps rating the severity of surface barriers and resembles, in an inverse manner, the procedure by Heinke and Kärger who correlated the surface permeability, α, with the diffusion coefficient, D.[5] Since $j^{\ddagger}_{surf} \propto \alpha$ and $j^{\ddagger}_{zeol} \propto D_S$, following relation holds

$$\delta_{crit} \propto \frac{j^{\ddagger}_{zeol}}{j^{\ddagger}_{surf}} \propto \left(\frac{\alpha}{D_S}\right)^{-1}. \tag{10}$$

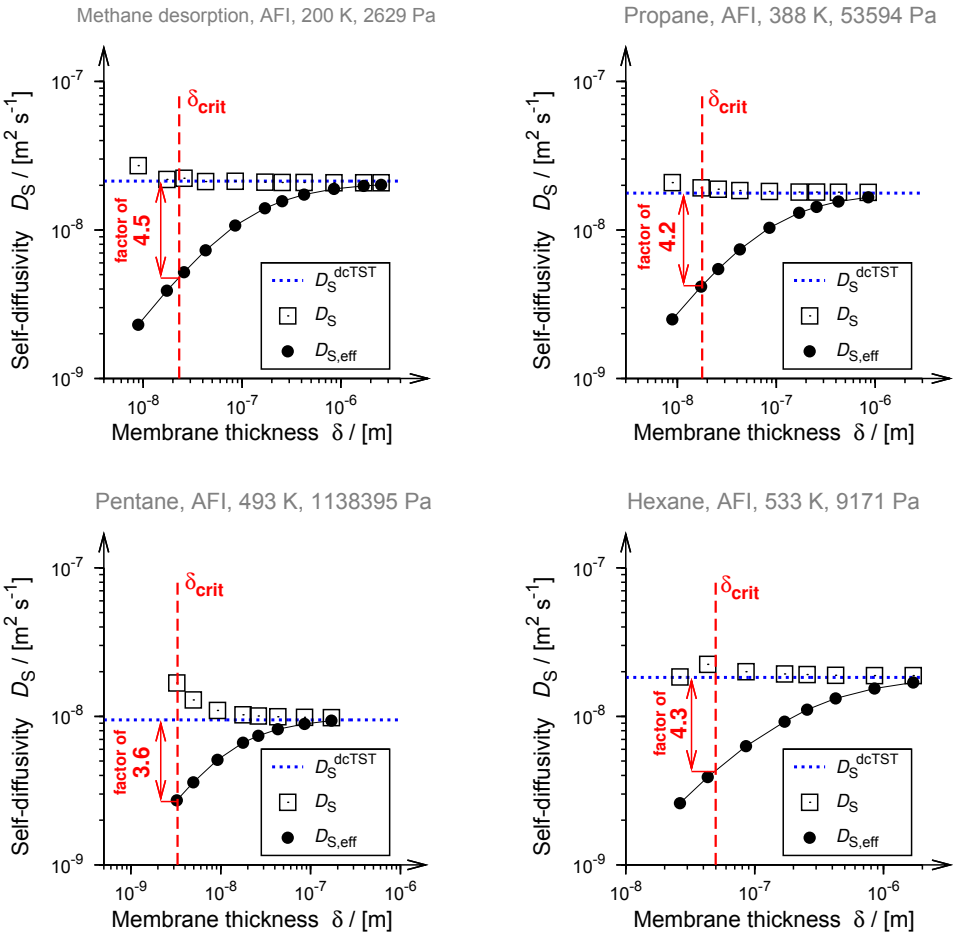

Figure S5: Increase of $D_{S,eff}$ with membrane thickness.

2 Isotherms and Heats of Adsorption

The adsorption isotherms of the hydrocarbon-zeolite systems, as obtained from GCMC simulations, are provided in Figure S6.

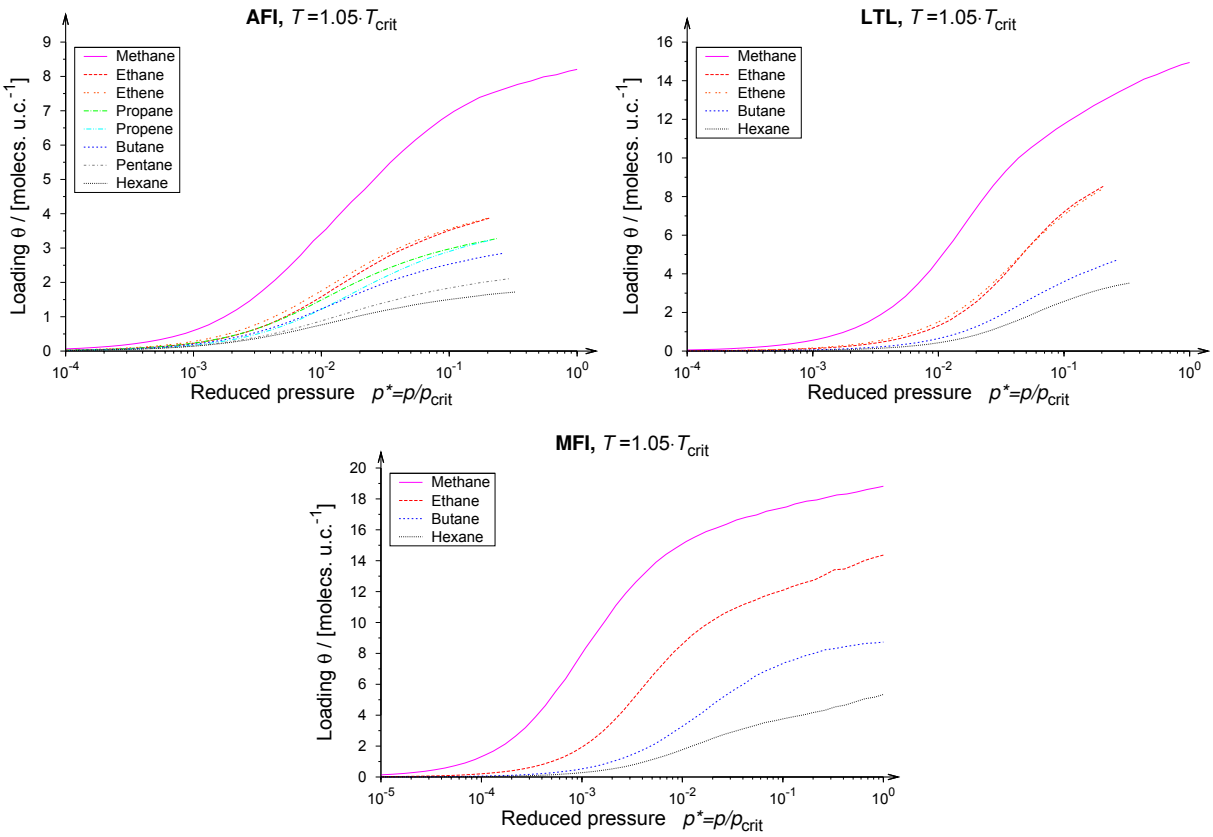

Figure S6: Isotherms from GCMC simulations in the fully periodic zeolites.

In Figure S7, the isosteric heats of adsorption obtained at zero loading in AFI are plotted over chain length of the molecule for two temperatures: 300 K and $1.05 \times T_{\text{crit}}$. Despite the fact that for hexane, for example, $1.05 \times T_{\text{crit}}$ is 233 K larger than 300 K (almost a factor of 2), the temperature has no evident influence on $-\Delta H_{\text{ads}}$. Also, the data of the *n*-alkanes and *n*-alkenes lie on a common trend line. Therefore, following linear function describes the dependence of the molecule's chain length on the heat of adsorption very well:

$$-\Delta H_{\text{ads}} = 7.21\ \text{kJ/mol} \times n + 7.21\ \text{kJ/mol}. \tag{11}$$

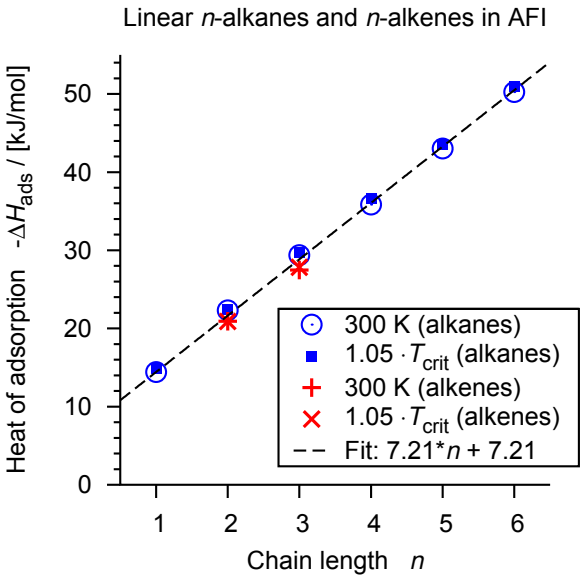

Figure S7: Isosteric heat of adsorption, $-\Delta H_{ads}$, at infinite dilution as a function of the molecule's chain length, n.

3 Transmission Coefficients

In Figure S8, the transmission coefficients in the boundary layers, κ_{surf}, of the 3 different zeolite membranes are plotted over loading, θ. Linear relationships between θ and κ_{surf} are observed in all cases. This was exploited to calculate the coefficients at zero loading (and thus zero pressure), see fitted lines in Figure S8.

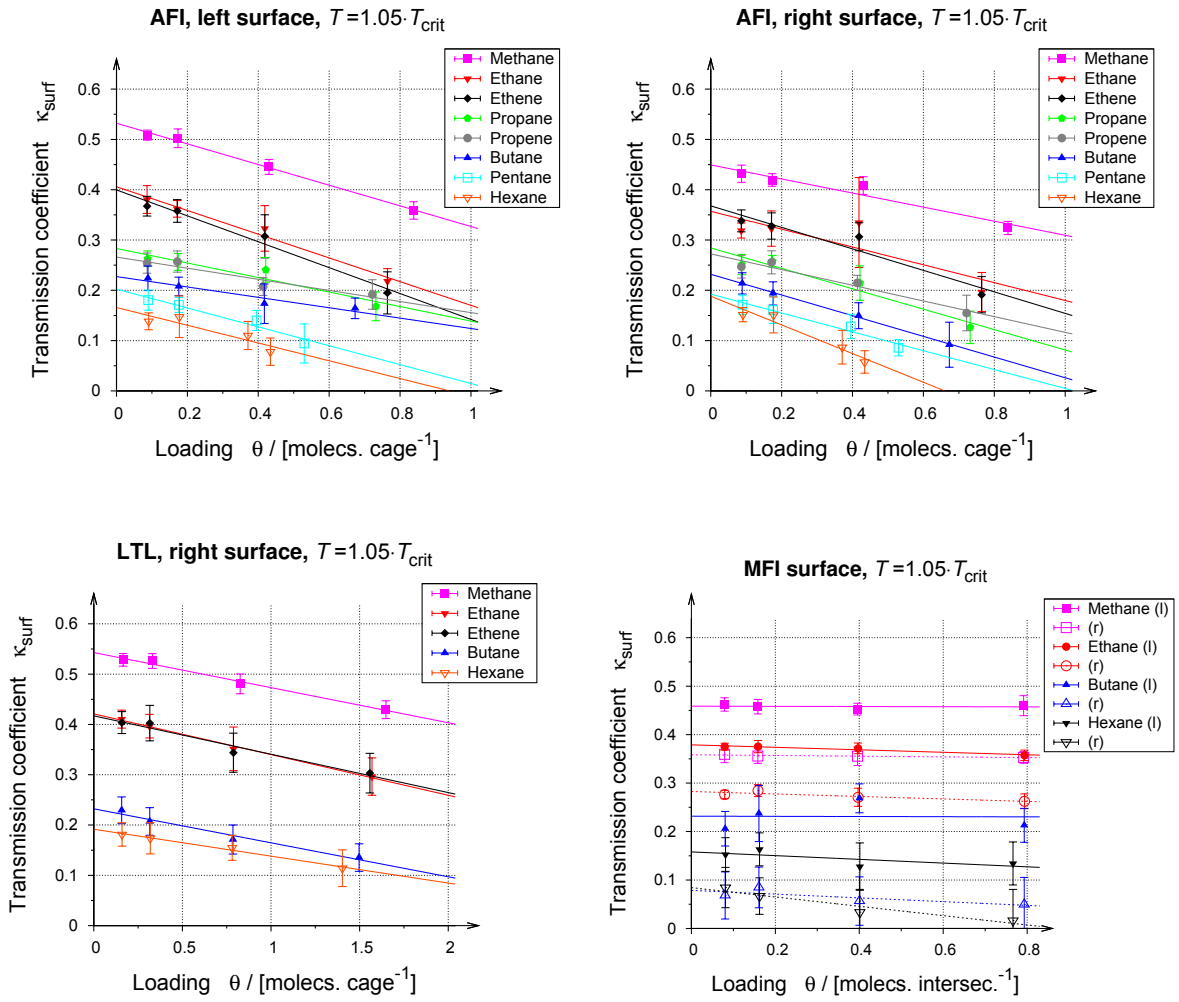

Figure S8: Transmission coefficients in zeolite boundary layer, κ_{surf}, *vs.* average loading, θ. From top left to bottom right: AFI window truncation, AFI cage truncation, LTL cage truncation, MFI left (l) and right (r) surface.

The transmission coefficient ratio (surface to bulk zeolite) remains constant with temperature, as can be seen from the examples given in Table S3. This justifies the simplified calculation of the

change in critical membrane thickness with temperature, as given in the main text, by just using the ratio of the respective histogram ratios:

$$\frac{\delta_{\mathrm{crit}}(T)}{\delta_{\mathrm{crit}}(T_{\mathrm{ref}})} = \frac{P^{\ddagger}_{\mathrm{zeol}}(T)/P^{\ddagger}_{\mathrm{surf}}(T)}{P^{\ddagger}_{\mathrm{zeol}}(T_{\mathrm{ref}})/P^{\ddagger}_{\mathrm{surf}}(T_{\mathrm{ref}})}. \tag{12}$$

In fact, the κ ratios do not vary much with neither temperature nor guest molecule type and surface nature.

TABLE S3: Transmission coefficients.[a]

	T	κ_{zeol}	$\kappa_{\mathrm{surf,l}}$	$\kappa_{\mathrm{surf,r}}$	$\kappa_{\mathrm{surf,l}}/\kappa_{\mathrm{zeol}}$	$\kappa_{\mathrm{surf,r}}/\kappa_{\mathrm{zeol}}$
	[K]	[–]	[–]	[–]	[–]	[–]
Methane	200	$1.005_{0.014}$	$0.528_{0.021}$	$0.463_{0.026}$	0.525	0.461
	300	$1.005_{0.064}$	$0.602_{0.026}$	$0.456_{0.028}$	0.599	0.454
Ethane	300	$0.623_{0.037}$	$0.378_{0.027}$	$0.305_{0.029}$	0.607	0.490
	321	$0.624_{0.018}$	$0.383_{0.035}$	$0.329_{0.029}$	0.614	0.527
Hexane	300	$0.280_{0.020}$	$0.142_{0.036}$	–[b]	0.507	–[b]
	533	$0.305_{0.019}$	$0.153_{0.028}$	$0.171_{0.028}$	0.502	0.561

[a] *Errors are given as subscripts .* [b] *No free-energy barrier appreciable.*

4 Critical Membrane Thickness – Remaining Surfaces

In Figure S9, critical membrane thicknesses obtained with the left, window-wise truncated AFI surface are displayed while in the main text the results for the right, cage-wise truncated AFI surface are presented. Differences between both diagrams are hardly detectable, justifying the conclusion that the surface structure does not significantly influence the transport in the AFI boundary layer.

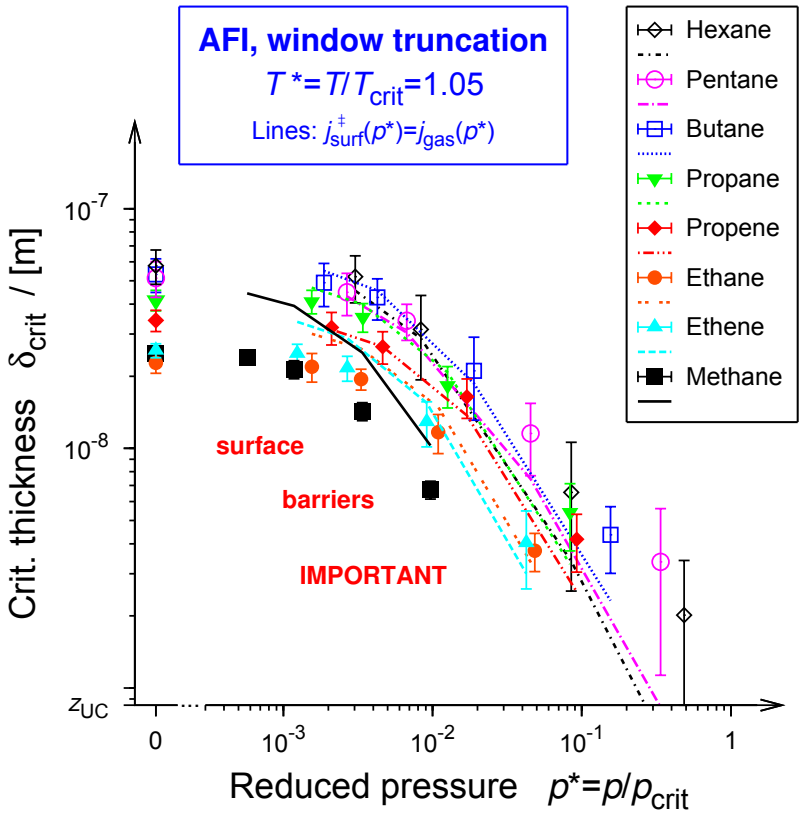

Figure S9: Critical membrane thickness, δ_{crit}, as a function of reduced pressure, $p^* = p/p_{\text{crit}}$, for different *n*-alkanes (C1-C6) and *n*-alkenes (C1-C2) adsorbed in all-silica AFI-type zeolites (membranes were truncated at the position of the window atoms). Note that (i) while the symbols represent *pure* simulation results, the lines are obtained by substituting $j^{\ddagger}_{\text{surf}}(p^*)$ with $j_{\text{gas}}(p^*)$ in Eq. (3) of main text, (ii) zero pressure corresponds to the limit where a single fluid molecule is found in the simulation box, and (iii) the lower range of the ordinate was set to the thickness of the AFI unit cell, z_{UC}.

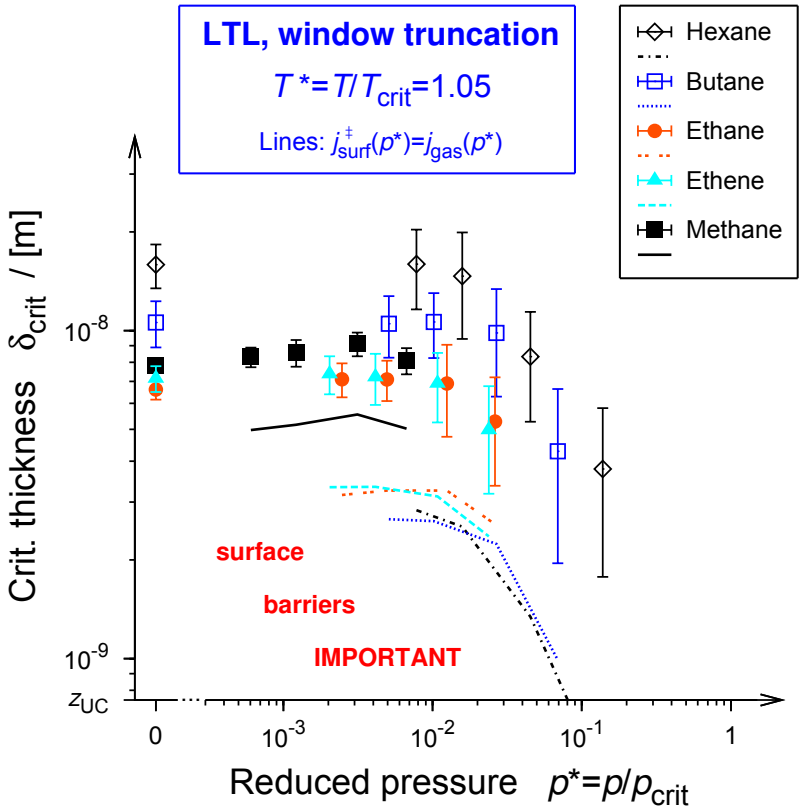

Figure S10: Critical membrane thickness, δ_{crit}, *vs.* reduced pressure, $p^* = p/p_{\text{crit}}$, for LTL (cf. Figure S9). The transmission coefficients at the left surface were approximated by those determined at the right surface. This is, $\kappa_{\text{surf,l}} = \kappa_{\text{surf,r}}$.

The LTL results obtained with the window-wise truncated surface (Figure S10) are not too different from the corresponding results presented in the main text either. Only, the "window" results are shifted up, roughly by a factor of two, which indicates that surface barriers in LTL are sensitive to the surface nature, in contrast to AFI. It, however, has to be pointed out that the results for LTL at the window-wise truncated membrane side are subject to an approximation, as discussed below.

The approximation made was that transmission coefficients at the left LTL surface were, for a given molecule and state point, assumed to be equal to the one calculated at the right boundary ($\kappa_{\text{surf,l}} = \kappa_{\text{surf,r}}$). The problem was the quite exceptional surface structure, see also Figure 1 in main text. The simple reaction coordinate (Cartesian z direction) did not describe the process of a guest molecule leaving the pore correctly. To explain this consider Figure S11, where a two-dimensional

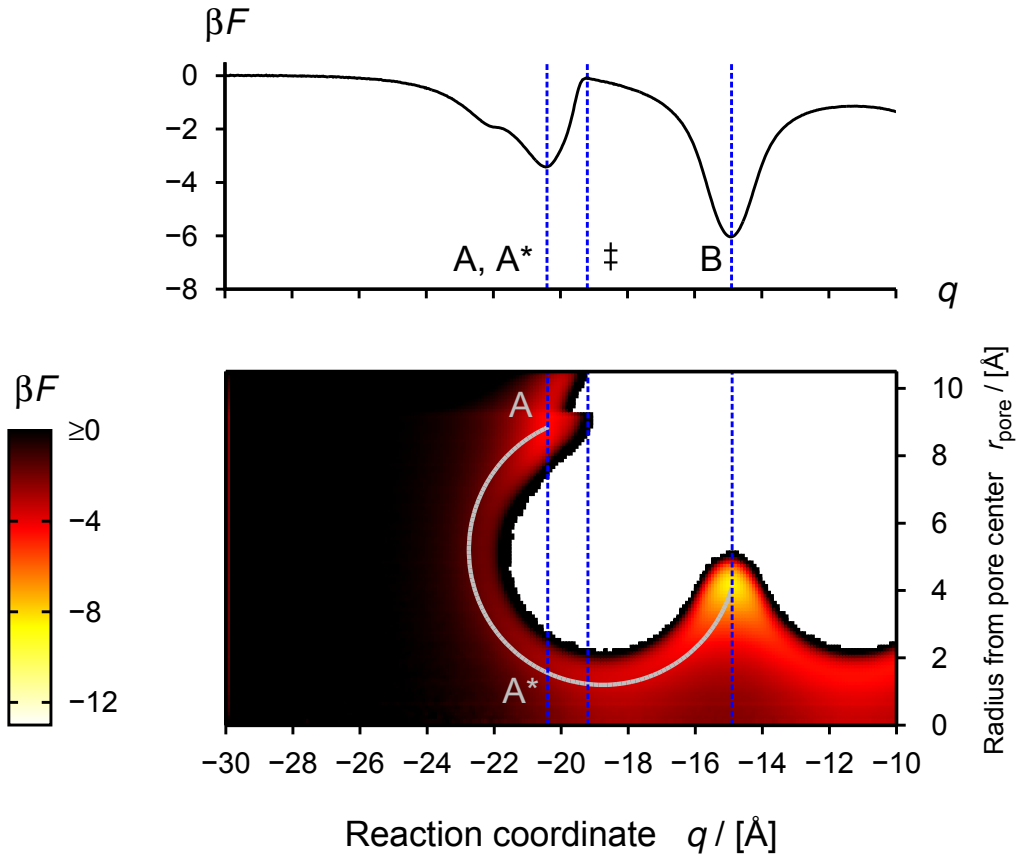

Figure S11: Top: One-dimensional free-energy profile, $\beta F(q)$. Bottom: Two-dimensional free-energy landscape, $\beta F(q, r_{\text{pore}})$. Methane around the window-wise truncated LTL surface (1 molecule, 200 K). The color box range was chosen such that white corresponds in fact to never visited regions.

free-energy landscape along with the corresponding 1D profile is shown for methane found in the vicinity of the left LTL pore mouth.

The dividing surface between crystal exterior (external surface plus gas region) and interior is located at $q^{\ddagger} = -19.2$ Å. The Cartesian reaction coordinate adequately describes a hop progress of the molecule from the barrier into the pore interior (first cage at $q_{\text{B}} = -14.9$ Å) because, between ‡ and B, there exist only one single region with respect to r_{pore} where residence is possible. This is yet not true for the opposite side. If a molecule attempts to move from ‡ along the minimum free-energy path toward A it has to first *cross* $q_{\text{A}} = -20.4$ Å once at A* ($r_{\text{pore}} \leq 3$ Å) to finally equilibrate in $[q_{\text{A}}, r_{\text{pore}} \sim 8$ Å$]$, being the true "stable state" for the "backward" reaction (out-of-

crystal jump). So, two separate regions of possible residence exist between A and ‡. Therefore, during the reactive flux simulation, a given shoot from $q^{\ddagger}$ that aims to the external surface will be stopped premature, if hop success is measured, without any additional order parameter, by the Cartesian reaction coordinate only, which was true in our simulations.

5 Temperature and Chain-Length Dependence of Henry Coefficient

In the main text, a coefficient X is used to correlate the change in critical membrane length with change in temperature, taking simultaneously into account the chain length of the molecules which, of course, exhibit different adsorption strengths. Here, it is shown how this coefficient was obtained and that it equals the change in Henry coefficient, K_{H}, with varying temperature, T, and chain length, n.

The starting point is the temperature dependence of the Henry coefficient for a given gas molecule (see, for example, Ref. 6):

$$\ln K_{\mathrm{H}}(T) = -\frac{\Delta H_{\mathrm{ads}}}{R} \cdot \frac{1}{T} - \mathrm{const.}, \tag{13}$$

where ΔH_{ads} denotes the isosteric heat of adsorption which is usually negative, R is the universal gas constant and T the temperature. The heat of adsorption can be expressed in terms of the molecule's chain length, n, as has been shown in Supporting Section 2:

$$-\Delta H_{\mathrm{ads}}(n) = a \cdot n + \Delta H_{\mathrm{ads},0}. \tag{14}$$

a and $\Delta H_{\mathrm{ads},0}$ are fitting parameters to the linear function, as determined earlier. Since the heat of adsorption does not change with temperature (Figure S7), Eq. (14) can be inserted into Eq. (13) and rearranged to:

$$K_{\mathrm{H}}(n,T) = \exp\left[\frac{a \cdot n + \Delta H_{\mathrm{ads},0}}{R} \cdot \frac{1}{T} - \mathrm{const.}\right]. \tag{15}$$

Defining T_{ref} as an (arbitrary) reference temperature, the ratio of the Henry coefficient at any temperature to its reference value at T_{ref} follows:

$$\frac{K_{\mathrm{H}}(n,T)}{K_{\mathrm{H}}(n,T_{\mathrm{ref}})} = \exp\left[\frac{a \cdot n + \Delta H_{\mathrm{ads},0}}{R} \cdot \left(\frac{1}{T} - \frac{1}{T_{\mathrm{ref}}}\right)\right] = X. \tag{16}$$

Hence, the coefficient X represents the analytical change in Henry coefficient with varying temperature by accounting for the length of the molecule, at the same time.

6 Crystal Structures

It was recently shown that molecular simulation results investigating tracer transport in zeolites are extremely sensitive to the crystal structure employed.[7]. Enhancing transparency and reproducibility, the unit cell structures used in the present work are given in the below subsections.

6.1 AFI

```
                                    23.774  13.726   8.484
                     90.000  90.000  90.000    SPGR =  1 P 1         OPT = 1
 144   0
    0 AFI         : AFI
   1 Si1      0.22620   0.10210   0.07800    5   7   9  11   0   0   0   0   0.000
   2 Si2      0.72620   0.60210   0.07800    6   8  10  12   0   0   0   0   0.000
   3 Si3     0.22885   0.10885   0.45000    7  83 101 117   0   0   0   0   0.000
   4 Si4     0.72885   0.60885   0.45000    8  84 102 118   0   0   0   0   0.000
   5 O5      0.21050   0.00320   0.02800    1   0   0   0   0   0   0   0   0.000
   6 O6      0.71050   0.50320   0.02800    2   0   0   0   0   0   0   0   0.000
   7 O7      0.22775   0.10345   0.25000    1   3   0   0   0   0   0   0   0.000
   8 O8      0.72775   0.60345   0.25000    2   4   0   0   0   0   0   0   0.000
   9 O9      0.18350   0.17490   0.02600    1   0   0   0   0   0   0   0   0.000
  10 O10     0.68350   0.67490   0.02600    2   0   0   0   0   0   0   0   0.000
  11 O11     0.28420   0.12840   0.01400    1   0   0   0   0   0   0   0   0.000
  12 O12     0.78420   0.62840   0.01400    2   0   0   0   0   0   0   0   0.000
  13 Si13     0.33585   0.78825   0.07800   17  19  21  23   0   0   0   0   0.000
  14 Si14     0.83585   0.28825   0.07800   18  20  22  24   0   0   0   0   0.000
  15 Si15    0.33115   0.78885   0.45000   19  89 107 141   0   0   0   0   0.000
  16 Si16    0.83115   0.28885   0.45000   20  90 108 142   0   0   0   0   0.000
  17 O17     0.39315   0.81415   0.02800   13   0   0   0   0   0   0   0   0.000
  18 O18     0.89315   0.31415   0.02800   14   0   0   0   0   0   0   0   0.000
  19 O19     0.33440   0.78990   0.25000   13  15   0   0   0   0   0   0   0.000
  20 O20     0.83440   0.28990   0.25000   14  16   0   0   0   0   0   0   0.000
  21 O21     0.32080   0.68780   0.02600   13   0   0   0   0   0   0   0   0.000
  22 O22     0.82080   0.18780   0.02600   14   0   0   0   0   0   0   0   0.000
  23 O23     0.29370   0.86210   0.01400   13   0   0   0   0   0   0   0   0.000
  24 O24     0.79370   0.36210   0.01400   14   0   0   0   0   0   0   0   0.000
  25 Si25     0.43795   0.10965   0.07800   29  31  33  35   0   0   0   0   0.000
  26 Si26     0.93795   0.60965   0.07800   30  32   0  36   0   0   0   0   0.000
  27 Si27    0.44000   0.10230   0.45000   31  77   0 130   0   0   0   0   0.000
```

28	Si28	0.94000	0.60230	0.45000	32	78	96	0	0	0	0	0	0.000
29	O29	0.39635	0.18265	0.02800	25	0	0	0	0	0	0	0	0.000
30	O30	0.89635	0.68265	0.02800	26	0	0	0	0	0	0	0	0.000
31	O31	0.43785	0.10665	0.25000	25	27	0	0	0	0	0	0	0.000
32	O32	0.93785	0.60665	0.25000	26	28	0	0	0	0	0	0	0.000
33	O33	0.49570	0.13730	0.02600	25	0	0	0	0	0	0	0	0.000
34	O34	-0.00430	0.63730	0.02600	0	0	0	0	0	0	0	0	0.000
35	O35	0.42210	0.00950	0.01400	25	0	0	0	0	0	0	0	0.000
36	O36	0.92210	0.50950	0.01400	26	0	0	0	0	0	0	0	0.000
37	Si37	0.27380	0.39790	0.07800	41	43	45	47	0	0	0	0	0.000
38	Si38	0.77380	0.89790	0.07800	0	44	46	48	0	0	0	0	0.000
39	Si39	0.27115	0.39115	0.45000	43	81	119	137	0	0	0	0	0.000
40	Si40	0.77115	0.89115	0.45000	44	82	120	0	0	0	0	0	0.000
41	O41	0.28950	0.49680	0.02800	37	0	0	0	0	0	0	0	0.000
42	O42	0.78950	-0.00320	0.02800	0	0	0	0	0	0	0	0	0.000
43	O43	0.27225	0.39655	0.25000	37	39	0	0	0	0	0	0	0.000
44	O44	0.77225	0.89655	0.25000	38	40	0	0	0	0	0	0	0.000
45	O45	0.31650	0.32510	0.02600	37	0	0	0	0	0	0	0	0.000
46	O46	0.81650	0.82510	0.02600	38	0	0	0	0	0	0	0	0.000
47	O47	0.21580	0.37160	0.01400	37	0	0	0	0	0	0	0	0.000
48	O48	0.71580	0.87160	0.01400	38	0	0	0	0	0	0	0	0.000
49	Si49	0.16415	0.71175	0.07800	53	55	57	59	0	0	0	0	0.000
50	Si50	0.66415	0.21175	0.07800	54	56	58	60	0	0	0	0	0.000
51	Si51	0.16885	0.71115	0.45000	55	105	125	143	0	0	0	0	0.000
52	Si52	0.66885	0.21115	0.45000	56	106	126	144	0	0	0	0	0.000
53	O53	0.10685	0.68585	0.02800	49	0	0	0	0	0	0	0	0.000
54	O54	0.60685	0.18585	0.02800	50	0	0	0	0	0	0	0	0.000
55	O55	0.16560	0.71010	0.25000	49	51	0	0	0	0	0	0	0.000
56	O56	0.66560	0.21010	0.25000	50	52	0	0	0	0	0	0	0.000
57	O57	0.17920	0.81220	0.02600	49	0	0	0	0	0	0	0	0.000
58	O58	0.67920	0.31220	0.02600	50	0	0	0	0	0	0	0	0.000
59	O59	0.20630	0.63790	0.01400	49	0	0	0	0	0	0	0	0.000
60	O60	0.70630	0.13790	0.01400	50	0	0	0	0	0	0	0	0.000
61	Si61	0.06205	0.39035	0.07800	65	67	69	71	0	0	0	0	0.000
62	Si62	0.56205	0.89035	0.07800	66	68	70	72	0	0	0	0	0.000
63	Si63	0.06000	0.39770	0.45000	67	94	113	131	0	0	0	0	0.000
64	Si64	0.56000	0.89770	0.45000	68	93	114	0	0	0	0	0	0.000
65	O65	0.10365	0.31735	0.02800	61	0	0	0	0	0	0	0	0.000
66	O66	0.60365	0.81735	0.02800	62	0	0	0	0	0	0	0	0.000
67	O67	0.06215	0.39335	0.25000	61	63	0	0	0	0	0	0	0.000
68	O68	0.56215	0.89335	0.25000	62	64	0	0	0	0	0	0	0.000

69	O69	0.00430	0.36270	0.02600	61	0	0	0	0	0	0	0	0.000
70	O70	0.50430	0.86270	0.02600	62	0	0	0	0	0	0	0	0.000
71	O71	0.07790	0.49050	0.01400	61	0	0	0	0	0	0	0	0.000
72	O72	0.57790	0.99050	0.01400	62	0	0	0	0	0	0	0	0.000
73	Si73	0.33585	0.21175	0.57800	77	79	81	83	0	0	0	0	0.000
74	Si74	0.83585	0.71175	0.57800	78	80	82	84	0	0	0	0	0.000
75	Si75	0.33115	0.21115	0.95000	0	0	0	79	0	0	0	0	0.000
76	Si76	0.83115	0.71115	0.95000	0	0	0	80	0	0	0	0	0.000
77	O77	0.39315	0.18585	0.52800	27	73	0	0	0	0	0	0	0.000
78	O78	0.89315	0.68585	0.52800	28	74	0	0	0	0	0	0	0.000
79	O79	0.33440	0.21010	0.75000	73	75	0	0	0	0	0	0	0.000
80	O80	0.83440	0.71010	0.75000	74	76	0	0	0	0	0	0	0.000
81	O81	0.32080	0.31220	0.52600	39	73	0	0	0	0	0	0	0.000
82	O82	0.82080	0.81220	0.52600	40	74	0	0	0	0	0	0	0.000
83	O83	0.29370	0.13790	0.51400	3	73	0	0	0	0	0	0	0.000
84	O84	0.79370	0.63790	0.51400	4	74	0	0	0	0	0	0	0.000
85	Si85	0.43795	0.89035	0.57800	89	91	93	95	0	0	0	0	0.000
86	Si86	0.93795	0.39035	0.57800	90	92	0	96	0	0	0	0	0.000
87	Si87	0.44000	0.89770	0.95000	0	0	0	91	0	0	0	0	0.000
88	Si88	0.94000	0.39770	0.95000	0	0	0	92	0	0	0	0	0.000
89	O89	0.39635	0.81735	0.52800	15	85	0	0	0	0	0	0	0.000
90	O90	0.89635	0.31735	0.52800	16	86	0	0	0	0	0	0	0.000
91	O91	0.43785	0.89335	0.75000	85	87	0	0	0	0	0	0	0.000
92	O92	0.93785	0.39335	0.75000	86	88	0	0	0	0	0	0	0.000
93	O93	0.49570	0.86270	0.52600	64	85	0	0	0	0	0	0	0.000
94	O94	-0.00430	0.36270	0.52600	63	0	0	0	0	0	0	0	0.000
95	O95	0.42210	0.99050	0.51400	0	85	0	0	0	0	0	0	0.000
96	O96	0.92210	0.49050	0.51400	28	86	0	0	0	0	0	0	0.000
97	Si97	0.22620	0.89790	0.57800	0	103	105	107	0	0	0	0	0.000
98	Si98	0.72620	0.39790	0.57800	102	104	106	108	0	0	0	0	0.000
99	Si99	0.22885	0.89115	0.95000	0	0	0	103	0	0	0	0	0.000
100	Si0	0.72885	0.39115	0.95000	0	0	0	104	0	0	0	0	0.000
101	O101	0.21050	-0.00320	0.52800	3	0	0	0	0	0	0	0	0.000
102	O102	0.71050	0.49680	0.52800	4	98	0	0	0	0	0	0	0.000
103	O103	0.22775	0.89655	0.75000	97	99	0	0	0	0	0	0	0.000
104	O104	0.72775	0.39655	0.75000	98	100	0	0	0	0	0	0	0.000
105	O105	0.18350	0.82510	0.52600	51	97	0	0	0	0	0	0	0.000
106	O106	0.68350	0.32510	0.52600	52	98	0	0	0	0	0	0	0.000
107	O107	0.28420	0.87160	0.51400	15	97	0	0	0	0	0	0	0.000
108	O108	0.78420	0.37160	0.51400	16	98	0	0	0	0	0	0	0.000
109	Si109	0.16415	0.28825	0.57800	113	115	117	119	0	0	0	0	0.000

```
110 Si110    0.66415   0.78825   0.57800  114 116 118 120   0   0   0   0   0.000
111 Si11    0.16885   0.28885   0.95000    0   0   0 115   0   0   0   0   0.000
112 Si12    0.66885   0.78885   0.95000    0   0   0 116   0   0   0   0   0.000
113 O113    0.10685   0.31415   0.52800   63 109   0   0   0   0   0   0   0.000
114 O114    0.60685   0.81415   0.52800   64 110   0   0   0   0   0   0   0.000
115 O115    0.16560   0.28990   0.75000  109 111   0   0   0   0   0   0   0.000
116 O116    0.66560   0.78990   0.75000  110 112   0   0   0   0   0   0   0.000
117 O117    0.17920   0.18780   0.52600    3 109   0   0   0   0   0   0   0.000
118 O118    0.67920   0.68780   0.52600    4 110   0   0   0   0   0   0   0.000
119 O119    0.20630   0.36210   0.51400   39 109   0   0   0   0   0   0   0.000
120 O120    0.70630   0.86210   0.51400   40 110   0   0   0   0   0   0   0.000
121 Si121    0.06205   0.60965   0.57800  125 127 129 131   0   0   0   0   0.000
122 Si122    0.56205   0.10965   0.57800  126 128 130 132   0   0   0   0   0.000
123 Si23    0.06000   0.60230   0.95000    0   0   0 127   0   0   0   0   0.000
124 Si24    0.56000   0.10230   0.95000    0   0   0 128   0   0   0   0   0.000
125 O125    0.10365   0.68265   0.52800   51 121   0   0   0   0   0   0   0.000
126 O126    0.60365   0.18265   0.52800   52 122   0   0   0   0   0   0   0.000
127 O127    0.06215   0.60665   0.75000  121 123   0   0   0   0   0   0   0.000
128 O128    0.56215   0.10665   0.75000  122 124   0   0   0   0   0   0   0.000
129 O129    0.00430   0.63730   0.52600    0 121   0   0   0   0   0   0   0.000
130 O130    0.50430   0.13730   0.52600   27 122   0   0   0   0   0   0   0.000
131 O131    0.07790   0.50950   0.51400   63 121   0   0   0   0   0   0   0.000
132 O132    0.57790   0.00950   0.51400    0 122   0   0   0   0   0   0   0.000
133 Si133    0.27380   0.60210   0.57800  137 139 141 143   0   0   0   0   0.000
134 Si134    0.77380   0.10210   0.57800  138 140 142 144   0   0   0   0   0.000
135 Si35    0.27115   0.60885   0.95000    0   0   0 139   0   0   0   0   0.000
136 Si36    0.77115   0.10885   0.95000    0   0   0 140   0   0   0   0   0.000
137 O137    0.28950   0.50320   0.52800   39 133   0   0   0   0   0   0   0.000
138 O138    0.78950   0.00320   0.52800    0 134   0   0   0   0   0   0   0.000
139 O139    0.27225   0.60345   0.75000  133 135   0   0   0   0   0   0   0.000
140 O140    0.77225   0.10345   0.75000  134 136   0   0   0   0   0   0   0.000
141 O141    0.31650   0.67490   0.52600   15 133   0   0   0   0   0   0   0.000
142 O142    0.81650   0.17490   0.52600   16 134   0   0   0   0   0   0   0.000
143 O143    0.21580   0.62840   0.51400   51 133   0   0   0   0   0   0   0.000
144 O144    0.71580   0.12840   0.51400   52 134   0   0   0   0   0   0   0.000
```

6.2 LTL

```
                                    31.984  18.466   7.476
                    90.000  90.000  90.000    SPGR =  1 P 1         OPT = 1
216   0
    0 LTL         : LTL
  1 Si1     0.04714   0.31122   0.50000    5   7  11 183   0   0   0   0   0.000
  2 Si2     0.54714   0.81122   0.50000    6   8  12 184   0   0   0   0   0.000
  3 Si3     0.08300   0.41592   0.21208    9  11  15  29   0   0   0   0   0.000
  4 Si4     0.58300   0.91592   0.21208   10  12  16   0   0   0   0   0   0.000
  5 O5      0.00000   0.27535   0.50000    1   0   0   0   0   0   0   0   0.000
  6 O6      0.50000   0.77535   0.50000    2 121   0   0   0   0   0   0   0.000
  7 O7      0.08294   0.24882   0.50000    1 145   0   0   0   0   0   0   0.000
  8 O8      0.58294   0.74882   0.50000    2 146   0   0   0   0   0   0   0.000
  9 O9      0.13283   0.39849   0.25604    3 197   0   0   0   0   0   0   0.000
 10 O10     0.63283   0.89849   0.25604    4 198   0   0   0   0   0   0   0.000
 11 O11     0.05111   0.36310   0.31828    1   3   0   0   0   0   0   0   0.000
 12 O12     0.55111   0.86310   0.31828    2   4   0   0   0   0   0   0   0.000
 13 O13     0.21255   0.63766   0.27509   35 193   0   0   0   0   0   0   0.000
 14 O14     0.71255   0.13766   0.27509   36 194   0   0   0   0   0   0   0.000
 15 O15     0.07208   0.40510   0.00000    3   0   0   0   0   0   0   0   0.000
 16 O16     0.57208   0.90510   0.00000    4   0   0   0   0   0   0   0   0.000
 17 Si17    0.32082   0.41509   0.50000   21  23  27 187   0   0   0   0   0.000
 18 Si18    0.82082   0.91509   0.50000   22   0  28 188   0   0   0   0   0.000
 19 Si19    0.25054   0.41654   0.21208   25  27  31  45   0   0   0   0   0.000
 20 Si20    0.75054   0.91654   0.21208    0  28  32  46   0   0   0   0   0.000
 21 O21     0.36232   0.36232   0.50000   17 109   0   0   0   0   0   0   0.000
 22 O22     0.86232   0.86232   0.50000   18 110   0   0   0   0   0   0   0.000
 23 O23     0.33412   0.50000   0.50000   17 133   0   0   0   0   0   0   0.000
 24 O24     0.83412   0.00000   0.50000    0 134   0   0   0   0   0   0   0.000
 25 O25     0.23434   0.50000   0.25604   19 193   0   0   0   0   0   0   0.000
 26 O26     0.73434   0.00000   0.25604    0 194   0   0   0   0   0   0   0.000
 27 O27     0.29289   0.39512   0.31828   17  19   0   0   0   0   0   0   0.000
 28 O28     0.79289   0.89512   0.31828   18  20   0   0   0   0   0   0   0.000
 29 O29     0.07489   0.50000   0.27509    3 201   0   0   0   0   0   0   0.000
 30 O30     0.57489   0.00000   0.27509    0 202   0   0   0   0   0   0   0.000
 31 O31     0.26141   0.40556   0.00000   19   0   0   0   0   0   0   0   0.000
 32 O32     0.76141   0.90556   0.00000   20   0   0   0   0   0   0   0   0.000
 33 Si33    0.13204   0.77369   0.50000   37  39  43 191   0   0   0   0   0.000
 34 Si34    0.63204   0.27369   0.50000   38  40  44 192   0   0   0   0   0.000
 35 Si35    0.16646   0.66754   0.21208   13  41  43  47   0   0   0   0   0.000
 36 Si36    0.66646   0.16754   0.21208   14  42  44  48   0   0   0   0   0.000
```

37 O37	0.13768	0.86232	0.50000	33	97	0	0	0	0	0	0	0.000
38 O38	0.63768	0.36232	0.50000	34	98	0	0	0	0	0	0	0.000
39 O39	0.08294	0.75118	0.50000	33	157	0	0	0	0	0	0	0.000
40 O40	0.58294	0.25118	0.50000	34	158	0	0	0	0	0	0	0.000
41 O41	0.13283	0.60151	0.25604	35	201	0	0	0	0	0	0	0.000
42 O42	0.63283	0.10151	0.25604	36	202	0	0	0	0	0	0	0.000
43 O43	0.15599	0.74178	0.31828	33	35	0	0	0	0	0	0	0.000
44 O44	0.65599	0.24178	0.31828	34	36	0	0	0	0	0	0	0.000
45 O45	0.21255	0.36234	0.27509	19	197	0	0	0	0	0	0	0.000
46 O46	0.71255	0.86234	0.27509	20	198	0	0	0	0	0	0	0.000
47 O47	0.16651	0.68934	0.00000	35	0	0	0	0	0	0	0	0.000
48 O48	0.66651	0.18934	0.00000	36	0	0	0	0	0	0	0	0.000
49 Si49	0.45286	0.18878	0.50000	54	55	59	171	0	0	0	0	0.000
50 Si50	0.95286	0.68878	0.50000	0	56	60	172	0	0	0	0	0.000
51 Si51	0.41700	0.08408	0.21208	57	59	63	77	0	0	0	0	0.000
52 Si52	0.91700	0.58408	0.21208	58	60	64	78	0	0	0	0	0.000
53 O53	0.00000	0.72465	0.50000	0	157	0	0	0	0	0	0	0.000
54 O54	0.50000	0.22465	0.50000	49	158	0	0	0	0	0	0	0.000
55 O55	0.41706	0.25118	0.50000	49	109	0	0	0	0	0	0	0.000
56 O56	0.91706	0.75118	0.50000	50	110	0	0	0	0	0	0	0.000
57 O57	0.36717	0.10151	0.25604	51	209	0	0	0	0	0	0	0.000
58 O58	0.86717	0.60151	0.25604	52	210	0	0	0	0	0	0	0.000
59 O59	0.44889	0.13690	0.31828	49	51	0	0	0	0	0	0	0.000
60 O60	0.94889	0.63690	0.31828	50	52	0	0	0	0	0	0	0.000
61 O61	0.28745	0.86234	0.27509	83	205	0	0	0	0	0	0	0.000
62 O62	0.78745	0.36234	0.27509	84	206	0	0	0	0	0	0	0.000
63 O63	0.42792	0.09490	0.00000	51	0	0	0	0	0	0	0	0.000
64 O64	0.92792	0.59490	0.00000	52	0	0	0	0	0	0	0	0.000
65 Si65	0.17918	0.08491	0.50000	69	71	75	175	0	0	0	0	0.000
66 Si66	0.67918	0.58491	0.50000	70	72	76	176	0	0	0	0	0.000
67 Si67	0.24946	0.08346	0.21208	73	75	79	93	0	0	0	0	0.000
68 Si68	0.74946	0.58346	0.21208	74	76	80	94	0	0	0	0	0.000
69 O69	0.13768	0.13768	0.50000	65	145	0	0	0	0	0	0	0.000
70 O70	0.63768	0.63768	0.50000	66	146	0	0	0	0	0	0	0.000
71 O71	0.16588	0.00000	0.50000	65	0	0	0	0	0	0	0	0.000
72 O72	0.66588	0.50000	0.50000	66	98	0	0	0	0	0	0	0.000
73 O73	0.26566	0.00000	0.25604	67	0	0	0	0	0	0	0	0.000
74 O74	0.76566	0.50000	0.25604	68	206	0	0	0	0	0	0	0.000
75 O75	0.20711	0.10488	0.31828	65	67	0	0	0	0	0	0	0.000
76 O76	0.70711	0.60488	0.31828	66	68	0	0	0	0	0	0	0.000
77 O77	0.42511	0.00000	0.27509	51	0	0	0	0	0	0	0	0.000

78	O78	0.92511	0.50000	0.27509	52	214	0	0	0	0	0	0	0.000
79	O79	0.23859	0.09444	0.00000	67	0	0	0	0	0	0	0	0.000
80	O80	0.73859	0.59444	0.00000	68	0	0	0	0	0	0	0	0.000
81	Si81	0.36796	0.72631	0.50000	85	87	91	179	0	0	0	0	0.000
82	Si82	0.86796	0.22631	0.50000	86	88	92	180	0	0	0	0	0.000
83	Si83	0.33354	0.83246	0.21208	61	89	91	95	0	0	0	0	0.000
84	Si84	0.83354	0.33246	0.21208	62	90	92	96	0	0	0	0	0.000
85	O85	0.36232	0.63768	0.50000	81	133	0	0	0	0	0	0	0.000
86	O86	0.86232	0.13768	0.50000	82	134	0	0	0	0	0	0	0.000
87	O87	0.41706	0.74882	0.50000	81	121	0	0	0	0	0	0	0.000
88	O88	0.91706	0.24882	0.50000	82	122	0	0	0	0	0	0	0.000
89	O89	0.36717	0.89849	0.25604	83	213	0	0	0	0	0	0	0.000
90	O90	0.86717	0.39849	0.25604	84	214	0	0	0	0	0	0	0.000
91	O91	0.34401	0.75822	0.31828	81	83	0	0	0	0	0	0	0.000
92	O92	0.84401	0.25822	0.31828	82	84	0	0	0	0	0	0	0.000
93	O93	0.28745	0.13766	0.27509	67	209	0	0	0	0	0	0	0.000
94	O94	0.78745	0.63766	0.27509	68	210	0	0	0	0	0	0	0.000
95	O95	0.33349	0.81066	0.00000	83	0	0	0	0	0	0	0	0.000
96	O96	0.83349	0.31066	0.00000	84	0	0	0	0	0	0	0	0.000
97	Si97	0.17918	0.91509	0.50000	37	0	103	207	0	0	0	0	0.000
98	Si98	0.67918	0.41509	0.50000	38	72	104	208	0	0	0	0	0.000
99	Si99	0.24946	0.91654	0.78792	0	103	0	117	0	0	0	0	0.000
100	Si0	0.74946	0.41654	0.78792	102	104	0	118	0	0	0	0	0.000
101	O101	0.26566	0.00000	0.74396	0	173	0	0	0	0	0	0	0.000
102	O102	0.76566	0.50000	0.74396	100	174	0	0	0	0	0	0	0.000
103	O103	0.20711	0.89512	0.68172	97	99	0	0	0	0	0	0	0.000
104	O104	0.70711	0.39512	0.68172	98	100	0	0	0	0	0	0	0.000
105	O105	0.42511	0.00000	0.72491	0	169	0	0	0	0	0	0	0.000
106	O106	0.92511	0.50000	0.72491	124	170	0	0	0	0	0	0	0.000
107	O107	0.23859	0.90556	0.00000	0	205	0	0	0	0	0	0	0.000
108	O108	0.73859	0.40556	0.00000	0	206	0	0	0	0	0	0	0.000
109	Si9	0.36796	0.27369	0.50000	21	55	115	211	0	0	0	0	0.000
110	Si10	0.86796	0.77369	0.50000	22	56	116	212	0	0	0	0	0.000
111	Si11	0.33354	0.16754	0.78792	113	115	0	129	0	0	0	0	0.000
112	Si12	0.83354	0.66754	0.78792	114	116	0	130	0	0	0	0	0.000
113	O113	0.36717	0.10151	0.74396	111	169	0	0	0	0	0	0	0.000
114	O114	0.86717	0.60151	0.74396	112	170	0	0	0	0	0	0	0.000
115	O115	0.34401	0.24178	0.68172	109	111	0	0	0	0	0	0	0.000
116	O116	0.84401	0.74178	0.68172	110	112	0	0	0	0	0	0	0.000
117	O117	0.28745	0.86234	0.72491	99	177	0	0	0	0	0	0	0.000
118	O118	0.78745	0.36234	0.72491	100	178	0	0	0	0	0	0	0.000

119	O119	0.33349	0.18934	0.00000	0	209	0	0	0	0	0	0	0.000
120	O120	0.83349	0.68934	0.00000	0	210	0	0	0	0	0	0	0.000
121	Si21	0.45286	0.81122	0.50000	6	87	127	215	0	0	0	0	0.000
122	Si22	0.95286	0.31122	0.50000	0	88	128	216	0	0	0	0	0.000
123	Si23	0.41700	0.91592	0.78792	0	125	127	0	0	0	0	0	0.000
124	Si24	0.91700	0.41592	0.78792	106	126	128	0	0	0	0	0	0.000
125	O125	0.36717	0.89849	0.74396	123	177	0	0	0	0	0	0	0.000
126	O126	0.86717	0.39849	0.74396	124	178	0	0	0	0	0	0	0.000
127	O127	0.44889	0.86310	0.68172	121	123	0	0	0	0	0	0	0.000
128	O128	0.94889	0.36310	0.68172	122	124	0	0	0	0	0	0	0.000
129	O129	0.28745	0.13766	0.72491	111	173	0	0	0	0	0	0	0.000
130	O130	0.78745	0.63766	0.72491	112	174	0	0	0	0	0	0	0.000
131	O131	0.42792	0.90510	0.00000	0	213	0	0	0	0	0	0	0.000
132	O132	0.92792	0.40510	0.00000	0	214	0	0	0	0	0	0	0.000
133	Si33	0.32082	0.58491	0.50000	23	85	139	195	0	0	0	0	0.000
134	Si34	0.82082	0.08491	0.50000	24	86	140	196	0	0	0	0	0.000
135	Si35	0.25054	0.58346	0.78792	137	139	0	153	0	0	0	0	0.000
136	Si36	0.75054	0.08346	0.78792	138	140	0	154	0	0	0	0	0.000
137	O137	0.23434	0.50000	0.74396	135	185	0	0	0	0	0	0	0.000
138	O138	0.73434	0.00000	0.74396	136	0	0	0	0	0	0	0	0.000
139	O139	0.29289	0.60488	0.68172	133	135	0	0	0	0	0	0	0.000
140	O140	0.79289	0.10488	0.68172	134	136	0	0	0	0	0	0	0.000
141	O141	0.07489	0.50000	0.72491	159	181	0	0	0	0	0	0	0.000
142	O142	0.57489	0.00000	0.72491	160	0	0	0	0	0	0	0	0.000
143	O143	0.26141	0.59444	0.00000	0	193	0	0	0	0	0	0	0.000
144	O144	0.76141	0.09444	0.00000	0	194	0	0	0	0	0	0	0.000
145	Si45	0.13204	0.22631	0.50000	7	69	151	199	0	0	0	0	0.000
146	Si46	0.63204	0.72631	0.50000	8	70	152	200	0	0	0	0	0.000
147	Si47	0.16646	0.33246	0.78792	149	151	0	165	0	0	0	0	0.000
148	Si48	0.66646	0.83246	0.78792	150	152	0	166	0	0	0	0	0.000
149	O149	0.13283	0.39849	0.74396	147	181	0	0	0	0	0	0	0.000
150	O150	0.63283	0.89849	0.74396	148	182	0	0	0	0	0	0	0.000
151	O151	0.15599	0.25822	0.68172	145	147	0	0	0	0	0	0	0.000
152	O152	0.65599	0.75822	0.68172	146	148	0	0	0	0	0	0	0.000
153	O153	0.21255	0.63766	0.72491	135	189	0	0	0	0	0	0	0.000
154	O154	0.71255	0.13766	0.72491	136	190	0	0	0	0	0	0	0.000
155	O155	0.16651	0.31066	0.00000	0	197	0	0	0	0	0	0	0.000
156	O156	0.66651	0.81066	0.00000	0	198	0	0	0	0	0	0	0.000
157	Si57	0.04714	0.68878	0.50000	39	53	163	203	0	0	0	0	0.000
158	Si58	0.54714	0.18878	0.50000	40	54	164	204	0	0	0	0	0.000
159	Si59	0.08300	0.58408	0.78792	141	161	163	0	0	0	0	0	0.000

160	Si60	0.58300	0.08408	0.78792	142	162	164	0	0	0	0	0	0.000
161	O161	0.13283	0.60151	0.74396	159	189	0	0	0	0	0	0	0.000
162	O162	0.63283	0.10151	0.74396	160	190	0	0	0	0	0	0	0.000
163	O163	0.05111	0.63690	0.68172	157	159	0	0	0	0	0	0	0.000
164	O164	0.55111	0.13690	0.68172	158	160	0	0	0	0	0	0	0.000
165	O165	0.21255	0.36234	0.72491	147	185	0	0	0	0	0	0	0.000
166	O166	0.71255	0.86234	0.72491	148	186	0	0	0	0	0	0	0.000
167	O167	0.07208	0.59490	0.00000	0	201	0	0	0	0	0	0	0.000
168	O168	0.57208	0.09490	0.00000	0	202	0	0	0	0	0	0	0.000
169	Si69	0.41700	0.08408	0.78792	0	105	113	171	0	0	0	0	0.000
170	Si70	0.91700	0.58408	0.78792	0	106	114	172	0	0	0	0	0.000
171	O171	0.44889	0.13690	0.68172	49	169	0	0	0	0	0	0	0.000
172	O172	0.94889	0.63690	0.68172	50	170	0	0	0	0	0	0	0.000
173	Si73	0.24946	0.08346	0.78792	0	101	129	175	0	0	0	0	0.000
174	Si74	0.74946	0.58346	0.78792	0	102	130	176	0	0	0	0	0.000
175	O175	0.20711	0.10488	0.68172	65	173	0	0	0	0	0	0	0.000
176	O176	0.70711	0.60488	0.68172	66	174	0	0	0	0	0	0	0.000
177	Si77	0.33354	0.83246	0.78792	0	117	125	179	0	0	0	0	0.000
178	Si78	0.83354	0.33246	0.78792	0	118	126	180	0	0	0	0	0.000
179	O179	0.34401	0.75822	0.68172	81	177	0	0	0	0	0	0	0.000
180	O180	0.84401	0.25822	0.68172	82	178	0	0	0	0	0	0	0.000
181	Si81	0.08300	0.41592	0.78792	0	141	149	183	0	0	0	0	0.000
182	Si82	0.58300	0.91592	0.78792	0	0	150	184	0	0	0	0	0.000
183	O183	0.05111	0.36310	0.68172	1	181	0	0	0	0	0	0	0.000
184	O184	0.55111	0.86310	0.68172	2	182	0	0	0	0	0	0	0.000
185	Si85	0.25054	0.41654	0.78792	0	137	165	187	0	0	0	0	0.000
186	Si86	0.75054	0.91654	0.78792	0	0	166	188	0	0	0	0	0.000
187	O187	0.29289	0.39512	0.68172	17	185	0	0	0	0	0	0	0.000
188	O188	0.79289	0.89512	0.68172	18	186	0	0	0	0	0	0	0.000
189	Si89	0.16646	0.66754	0.78792	0	153	161	191	0	0	0	0	0.000
190	Si90	0.66646	0.16754	0.78792	0	154	162	192	0	0	0	0	0.000
191	O191	0.15599	0.74178	0.68172	33	189	0	0	0	0	0	0	0.000
192	O192	0.65599	0.24178	0.68172	34	190	0	0	0	0	0	0	0.000
193	Si93	0.25054	0.58346	0.21208	13	25	143	195	0	0	0	0	0.000
194	Si94	0.75054	0.08346	0.21208	14	26	144	196	0	0	0	0	0.000
195	O195	0.29289	0.60488	0.31828	133	193	0	0	0	0	0	0	0.000
196	O196	0.79289	0.10488	0.31828	134	194	0	0	0	0	0	0	0.000
197	Si97	0.16646	0.33246	0.21208	9	45	155	199	0	0	0	0	0.000
198	Si98	0.66646	0.83246	0.21208	10	46	156	200	0	0	0	0	0.000
199	O199	0.15599	0.25822	0.31828	145	197	0	0	0	0	0	0	0.000
200	O200	0.65599	0.75822	0.31828	146	198	0	0	0	0	0	0	0.000

201	Si1	0.08300	0.58408	0.21208	29	41	167	203	0	0	0	0	0.000
202	Si2	0.58300	0.08408	0.21208	30	42	168	204	0	0	0	0	0.000
203	O203	0.05111	0.63690	0.31828	157	201	0	0	0	0	0	0	0.000
204	O204	0.55111	0.13690	0.31828	158	202	0	0	0	0	0	0	0.000
205	Si5	0.24946	0.91654	0.21208	61	0	107	207	0	0	0	0	0.000
206	Si6	0.74946	0.41654	0.21208	62	74	108	208	0	0	0	0	0.000
207	O207	0.20711	0.89512	0.31828	97	205	0	0	0	0	0	0	0.000
208	O208	0.70711	0.39512	0.31828	98	206	0	0	0	0	0	0	0.000
209	Si9	0.33354	0.16754	0.21208	57	93	119	211	0	0	0	0	0.000
210	Si10	0.83354	0.66754	0.21208	58	94	120	212	0	0	0	0	0.000
211	O211	0.34401	0.24178	0.31828	109	209	0	0	0	0	0	0	0.000
212	O212	0.84401	0.74178	0.31828	110	210	0	0	0	0	0	0	0.000
213	Si13	0.41700	0.91592	0.21208	0	89	131	215	0	0	0	0	0.000
214	Si14	0.91700	0.41592	0.21208	78	90	132	216	0	0	0	0	0.000
215	O215	0.44889	0.86310	0.31828	121	213	0	0	0	0	0	0	0.000
216	O216	0.94889	0.36310	0.31828	122	214	0	0	0	0	0	0	0.000

6.3 MFI

```
                                    20.022  19.899  13.383
                    90.000  90.000  90.000    SPGR =  1 P 1         OPT = 1
288   0
    0 MFI         : MFI
  1 Si1     0.42238   0.05650   0.66402   13  27  28 219   0   0   0   0   0.000
  2 Si2     0.30716   0.02772   0.81070   13  14  18   0   0   0   0   0   0.000
  3 Si3     0.27911   0.06127   0.03120    0  15  69  70   0   0   0   0   0.000
  4 Si4     0.12215   0.06298   0.02670   15   0  66  67   0   0   0   0   0.000
  5 Si5     0.07128   0.02722   0.81449   16  17   0   0   0   0   0   0   0.000
  6 Si6     0.18641   0.05896   0.67182   17  18  30  31   0   0   0   0   0.000
  7 Si7     0.42265   0.82750   0.67282   19  29  35 220   0   0   0   0   0.000
  8 Si8     0.30778   0.86984   0.81452   19  20  24  25   0   0   0   0   0.000
  9 Si9     0.27554   0.82721   0.03109    0  21  37  68   0   0   0   0   0.000
 10 Si10    0.12058   0.82690   0.02979   21   0  38  65   0   0   0   0   0.000
 11 Si11    0.07044   0.86963   0.81800   22  23  26   0   0   0   0   0   0.000
 12 Si12    0.18706   0.82673   0.68067   23  24  32  36   0   0   0   0   0.000
 13 O13     0.37260   0.05340   0.75580    1   2   0   0   0   0   0   0   0.000
 14 O14     0.30840   0.05870   0.92110    2   0   0   0   0   0   0   0   0.000
 15 O15     0.20070   0.05920   0.02890    3   4   0   0   0   0   0   0   0.000
 16 O16     0.09690   0.06110   0.91440    0   5   0   0   0   0   0   0   0.000
 17 O17     0.11490   0.05410   0.72370    5   6   0   0   0   0   0   0   0.000
 18 O18     0.24350   0.05530   0.75400    2   6   0   0   0   0   0   0   0.000
 19 O19     0.37420   0.84390   0.76280    7   8   0   0   0   0   0   0   0.000
 20 O20     0.30850   0.84480   0.92720    8   0   0   0   0   0   0   0   0.000
 21 O21     0.19800   0.84460   0.02880    9  10   0   0   0   0   0   0   0.000
 22 O22     0.09100   0.83860   0.92230    0  11   0   0   0   0   0   0   0.000
 23 O23     0.11690   0.84220   0.73060   11  12   0   0   0   0   0   0   0.000
 24 O24     0.24480   0.84060   0.75780    8  12   0   0   0   0   0   0   0.000
 25 O25     0.30470   0.94900   0.81340    0   8   0   0   0   0   0   0   0.000
 26 O26     0.07680   0.94810   0.82310    0  11   0   0   0   0   0   0   0.000
 27 O27     0.41610   0.12760   0.61040    1  48   0   0   0   0   0   0   0.000
 28 O28     0.40860  -0.00170   0.58640    1   0   0   0   0   0   0   0   0.000
 29 O29     0.40200   0.86860   0.57610    7  42   0   0   0   0   0   0   0.000
 30 O30     0.18860   0.12980   0.61640    6  47   0   0   0   0   0   0   0.000
 31 O31     0.19400   0.00070   0.59180    6   0   0   0   0   0   0   0   0.000
 32 O32     0.19510   0.87090   0.58100   12  41   0   0   0   0   0   0   0.000
 33 O33     0.99600   0.04250   0.79220    0 187   0   0   0   0   0   0   0.000
 34 O34     0.99600   0.84720   0.79220    0 193   0   0   0   0   0   0   0.000
 35 O35     0.41920   0.75000   0.64600    7 227   0   0   0   0   0   0   0.000
 36 O36     0.18840   0.75000   0.64620   12 232   0   0   0   0   0   0   0.000
```

37	O37	0.28830	0.75000	0.05790	9	229	0	0	0	0	0	0	0.000
38	O38	0.10850	0.75000	0.06110	10	230	0	0	0	0	0	0	0.000
39	Si39	0.07762	0.94350	0.16402	51	65	0	185	0	0	0	0	0.000
40	Si40	0.19284	0.97228	0.31070	51	52	56	0	0	0	0	0	0.000
41	Si41	0.22089	0.93873	0.53120	0	32	52	53	0	0	0	0	0.000
42	Si42	0.37785	0.93702	0.52670	0	29	53	54	0	0	0	0	0.000
43	Si43	0.42872	0.97278	0.31449	54	55	0	71	0	0	0	0	0.000
44	Si44	0.31359	0.94104	0.17182	55	56	68	0	0	0	0	0	0.000
45	Si45	0.07735	0.17250	0.17282	57	67	73	186	0	0	0	0	0.000
46	Si46	0.19222	0.13016	0.31452	57	58	62	63	0	0	0	0	0.000
47	Si47	0.22446	0.17279	0.53109	30	58	59	75	0	0	0	0	0.000
48	Si48	0.37942	0.17310	0.52979	27	59	60	76	0	0	0	0	0.000
49	Si49	0.42956	0.13037	0.31800	60	61	64	72	0	0	0	0	0.000
50	Si50	0.31294	0.17327	0.18067	61	62	70	74	0	0	0	0	0.000
51	O51	0.12740	0.94660	0.25580	39	40	0	0	0	0	0	0	0.000
52	O52	0.19160	0.94130	0.42110	40	41	0	0	0	0	0	0	0.000
53	O53	0.29930	0.94080	0.52890	41	42	0	0	0	0	0	0	0.000
54	O54	0.40310	0.93890	0.41440	42	43	0	0	0	0	0	0	0.000
55	O55	0.38510	0.94590	0.22370	43	44	0	0	0	0	0	0	0.000
56	O56	0.25650	0.94470	0.25400	40	44	0	0	0	0	0	0	0.000
57	O57	0.12580	0.15610	0.26280	45	46	0	0	0	0	0	0	0.000
58	O58	0.19150	0.15520	0.42720	46	47	0	0	0	0	0	0	0.000
59	O59	0.30200	0.15540	0.52880	47	48	0	0	0	0	0	0	0.000
60	O60	0.40900	0.16140	0.42230	48	49	0	0	0	0	0	0	0.000
61	O61	0.38310	0.15780	0.23060	49	50	0	0	0	0	0	0	0.000
62	O62	0.25520	0.15940	0.25780	46	50	0	0	0	0	0	0	0.000
63	O63	0.19530	0.05100	0.31340	0	46	0	0	0	0	0	0	0.000
64	O64	0.42320	0.05190	0.32310	0	49	0	0	0	0	0	0	0.000
65	O65	0.08390	0.87240	0.11040	10	39	0	0	0	0	0	0	0.000
66	O66	0.09140	0.00170	0.08640	4	0	0	0	0	0	0	0	0.000
67	O67	0.09800	0.13140	0.07610	4	45	0	0	0	0	0	0	0.000
68	O68	0.31140	0.87020	0.11640	9	44	0	0	0	0	0	0	0.000
69	O69	0.30600	-0.00070	0.09180	3	0	0	0	0	0	0	0	0.000
70	O70	0.30490	0.12910	0.08100	3	50	0	0	0	0	0	0	0.000
71	O71	0.50400	0.95750	0.29220	43	153	0	0	0	0	0	0	0.000
72	O72	0.50400	0.15280	0.29220	49	159	0	0	0	0	0	0	0.000
73	O73	0.08080	0.25000	0.14600	45	261	0	0	0	0	0	0	0.000
74	O74	0.31160	0.25000	0.14620	50	266	0	0	0	0	0	0	0.000
75	O75	0.21170	0.25000	0.55790	47	263	0	0	0	0	0	0	0.000
76	O76	0.39150	0.25000	0.56110	48	264	0	0	0	0	0	0	0.000
77	Si77	0.57762	0.55650	0.33598	89	103	104	287	0	0	0	0	0.000

78	Si78	0.69284	0.52772	0.18930	89	90	94	101	0	0	0	0	0.000
79	Si79	0.72089	0.56127	0.96880	0	91	145	146	0	0	0	0	0.000
80	Si80	0.87785	0.56298	0.97330	91	0	142	143	0	0	0	0	0.000
81	Si81	0.92872	0.52722	0.18551	92	93	102	0	0	0	0	0	0.000
82	Si82	0.81359	0.55896	0.32818	93	94	106	107	0	0	0	0	0.000
83	Si83	0.57735	0.32750	0.32718	95	105	111	288	0	0	0	0	0.000
84	Si84	0.69222	0.36984	0.18548	95	96	100	101	0	0	0	0	0.000
85	Si85	0.72446	0.32721	0.96891	0	97	113	144	0	0	0	0	0.000
86	Si86	0.87942	0.32690	0.97021	97	0	114	141	0	0	0	0	0.000
87	Si87	0.92956	0.36963	0.18200	98	99	102	0	0	0	0	0	0.000
88	Si88	0.81294	0.32673	0.31933	99	100	108	112	0	0	0	0	0.000
89	O89	0.62740	0.55340	0.24420	77	78	0	0	0	0	0	0	0.000
90	O90	0.69160	0.55870	0.07890	78	0	0	0	0	0	0	0	0.000
91	O91	0.79930	0.55920	0.97110	79	80	0	0	0	0	0	0	0.000
92	O92	0.90310	0.56110	0.08560	0	81	0	0	0	0	0	0	0.000
93	O93	0.88510	0.55410	0.27630	81	82	0	0	0	0	0	0	0.000
94	O94	0.75650	0.55530	0.24600	78	82	0	0	0	0	0	0	0.000
95	O95	0.62580	0.34390	0.23720	83	84	0	0	0	0	0	0	0.000
96	O96	0.69150	0.34480	0.07280	84	0	0	0	0	0	0	0	0.000
97	O97	0.80200	0.34460	0.97120	85	86	0	0	0	0	0	0	0.000
98	O98	0.90900	0.33860	0.07770	0	87	0	0	0	0	0	0	0.000
99	O99	0.88310	0.34220	0.26940	87	88	0	0	0	0	0	0	0.000
100	O100	0.75520	0.34060	0.24220	84	88	0	0	0	0	0	0	0.000
101	O101	0.69530	0.44900	0.18660	78	84	0	0	0	0	0	0	0.000
102	O102	0.92320	0.44810	0.17690	81	87	0	0	0	0	0	0	0.000
103	O103	0.58390	0.62760	0.38960	77	124	0	0	0	0	0	0	0.000
104	O104	0.59140	0.49830	0.41360	77	118	0	0	0	0	0	0	0.000
105	O105	0.59800	0.36860	0.42390	83	118	0	0	0	0	0	0	0.000
106	O106	0.81140	0.62980	0.38360	82	123	0	0	0	0	0	0	0.000
107	O107	0.80600	0.50070	0.40820	82	117	0	0	0	0	0	0	0.000
108	O108	0.80490	0.37090	0.41900	88	117	0	0	0	0	0	0	0.000
109	O109	0.00400	0.54250	0.20780	0	255	0	0	0	0	0	0	0.000
110	O110	0.00400	0.34720	0.20780	0	261	0	0	0	0	0	0	0.000
111	O111	0.58080	0.25000	0.35400	83	159	0	0	0	0	0	0	0.000
112	O112	0.81160	0.25000	0.35380	88	164	0	0	0	0	0	0	0.000
113	O113	0.71170	0.25000	0.94210	85	161	0	0	0	0	0	0	0.000
114	O114	0.89150	0.25000	0.93890	86	162	0	0	0	0	0	0	0.000
115	Si15	0.92238	0.44350	0.83598	127	141	142	253	0	0	0	0	0.000
116	Si16	0.80716	0.47228	0.68930	127	128	132	139	0	0	0	0	0.000
117	Si17	0.77911	0.43873	0.46880	107	108	128	129	0	0	0	0	0.000
118	Si18	0.62215	0.43702	0.47330	104	105	129	130	0	0	0	0	0.000

119	Si19	0.57128	0.47278	0.68551	130	131	140	147	0	0	0	0	0.000
120	Si20	0.68641	0.44104	0.82818	131	132	144	145	0	0	0	0	0.000
121	Si21	0.92265	0.67250	0.82718	133	143	149	254	0	0	0	0	0.000
122	Si22	0.80778	0.63016	0.68548	133	134	138	139	0	0	0	0	0.000
123	Si23	0.77554	0.67279	0.46891	106	134	135	151	0	0	0	0	0.000
124	Si24	0.62058	0.67310	0.47021	103	135	136	152	0	0	0	0	0.000
125	Si25	0.57044	0.63037	0.68200	136	137	140	148	0	0	0	0	0.000
126	Si26	0.68706	0.67327	0.81933	137	138	146	150	0	0	0	0	0.000
127	O127	0.87260	0.44660	0.74420	115	116	0	0	0	0	0	0	0.000
128	O128	0.80840	0.44130	0.57890	116	117	0	0	0	0	0	0	0.000
129	O129	0.70070	0.44080	0.47110	117	118	0	0	0	0	0	0	0.000
130	O130	0.59690	0.43890	0.58560	118	119	0	0	0	0	0	0	0.000
131	O131	0.61490	0.44590	0.77630	119	120	0	0	0	0	0	0	0.000
132	O132	0.74350	0.44470	0.74600	116	120	0	0	0	0	0	0	0.000
133	O133	0.87420	0.65610	0.73720	121	122	0	0	0	0	0	0	0.000
134	O134	0.80850	0.65520	0.57280	122	123	0	0	0	0	0	0	0.000
135	O135	0.69800	0.65540	0.47120	123	124	0	0	0	0	0	0	0.000
136	O136	0.59100	0.66140	0.57770	124	125	0	0	0	0	0	0	0.000
137	O137	0.61690	0.65780	0.76940	125	126	0	0	0	0	0	0	0.000
138	O138	0.74480	0.65940	0.74220	122	126	0	0	0	0	0	0	0.000
139	O139	0.80470	0.55100	0.68660	116	122	0	0	0	0	0	0	0.000
140	O140	0.57680	0.55190	0.67690	119	125	0	0	0	0	0	0	0.000
141	O141	0.91610	0.37240	0.88960	86	115	0	0	0	0	0	0	0.000
142	O142	0.90860	0.50170	0.91360	80	115	0	0	0	0	0	0	0.000
143	O143	0.90200	0.63140	0.92390	80	121	0	0	0	0	0	0	0.000
144	O144	0.68860	0.37020	0.88360	85	120	0	0	0	0	0	0	0.000
145	O145	0.69400	0.49930	0.90820	79	120	0	0	0	0	0	0	0.000
146	O146	0.69510	0.62910	0.91900	79	126	0	0	0	0	0	0	0.000
147	O147	0.49600	0.45750	0.70780	119	221	0	0	0	0	0	0	0.000
148	O148	0.49600	0.65280	0.70780	125	227	0	0	0	0	0	0	0.000
149	O149	0.91920	0.75000	0.85400	121	193	0	0	0	0	0	0	0.000
150	O150	0.68840	0.75000	0.85380	126	198	0	0	0	0	0	0	0.000
151	O151	0.78830	0.75000	0.44210	123	195	0	0	0	0	0	0	0.000
152	O152	0.60850	0.75000	0.43890	124	196	0	0	0	0	0	0	0.000
153	Si53	0.57762	0.94350	0.33598	71	165	179	0	0	0	0	0	0.000
154	Si54	0.69284	0.97228	0.18930	165	166	170	0	0	0	0	0	0.000
155	Si55	0.72089	0.93873	0.96880	0	167	0	218	0	0	0	0	0.000
156	Si56	0.87785	0.93702	0.97330	167	0	0	215	0	0	0	0	0.000
157	Si57	0.92872	0.97278	0.18551	168	169	0	0	0	0	0	0	0.000
158	Si58	0.81359	0.94104	0.32818	169	170	182	0	0	0	0	0	0.000
159	Si59	0.57735	0.17250	0.32718	72	111	171	181	0	0	0	0	0.000

160	Si60	0.69222	0.13016	0.18548	171	172	176	177	0	0	0	0	0.000
161	Si61	0.72446	0.17279	0.96891	113	0	173	216	0	0	0	0	0.000
162	Si62	0.87942	0.17310	0.97021	114	173	0	213	0	0	0	0	0.000
163	Si63	0.92956	0.13037	0.18200	174	175	178	0	0	0	0	0	0.000
164	Si64	0.81294	0.17327	0.31933	112	175	176	184	0	0	0	0	0.000
165	O165	0.62740	0.94660	0.24420	153	154	0	0	0	0	0	0	0.000
166	O166	0.69160	0.94130	0.07890	154	0	0	0	0	0	0	0	0.000
167	O167	0.79930	0.94080	0.97110	155	156	0	0	0	0	0	0	0.000
168	O168	0.90310	0.93890	0.08560	0	157	0	0	0	0	0	0	0.000
169	O169	0.88510	0.94590	0.27630	157	158	0	0	0	0	0	0	0.000
170	O170	0.75650	0.94470	0.24600	154	158	0	0	0	0	0	0	0.000
171	O171	0.62580	0.15610	0.23720	159	160	0	0	0	0	0	0	0.000
172	O172	0.69150	0.15520	0.07280	160	0	0	0	0	0	0	0	0.000
173	O173	0.80200	0.15540	0.97120	161	162	0	0	0	0	0	0	0.000
174	O174	0.90900	0.16140	0.07770	0	163	0	0	0	0	0	0	0.000
175	O175	0.88310	0.15780	0.26940	163	164	0	0	0	0	0	0	0.000
176	O176	0.75520	0.15940	0.24220	160	164	0	0	0	0	0	0	0.000
177	O177	0.69530	0.05100	0.18660	0	160	0	0	0	0	0	0	0.000
178	O178	0.92320	0.05190	0.17690	0	163	0	0	0	0	0	0	0.000
179	O179	0.58390	0.87240	0.38960	153	196	0	0	0	0	0	0	0.000
180	O180	0.59140	0.00170	0.41360	0	190	0	0	0	0	0	0	0.000
181	O181	0.59800	0.13140	0.42390	159	190	0	0	0	0	0	0	0.000
182	O182	0.81140	0.87020	0.38360	158	195	0	0	0	0	0	0	0.000
183	O183	0.80600	-0.00070	0.40820	0	189	0	0	0	0	0	0	0.000
184	O184	0.80490	0.12910	0.41900	164	189	0	0	0	0	0	0	0.000
185	O185	0.00400	0.95750	0.20780	39	0	0	0	0	0	0	0	0.000
186	O186	0.00400	0.15280	0.20780	45	0	0	0	0	0	0	0	0.000
187	Si87	0.92238	0.05650	0.83598	33	199	213	214	0	0	0	0	0.000
188	Si88	0.80716	0.02772	0.68930	199	200	204	0	0	0	0	0	0.000
189	Si89	0.77911	0.06127	0.46880	183	184	200	201	0	0	0	0	0.000
190	Si90	0.62215	0.06298	0.47330	180	181	201	202	0	0	0	0	0.000
191	Si91	0.57128	0.02722	0.68551	202	203	0	219	0	0	0	0	0.000
192	Si92	0.68641	0.05896	0.82818	203	204	216	217	0	0	0	0	0.000
193	Si93	0.92265	0.82750	0.82718	34	149	205	215	0	0	0	0	0.000
194	Si94	0.80778	0.86984	0.68548	205	206	210	211	0	0	0	0	0.000
195	Si95	0.77554	0.82721	0.46891	151	182	206	207	0	0	0	0	0.000
196	Si96	0.62058	0.82690	0.47021	152	179	207	208	0	0	0	0	0.000
197	Si97	0.57044	0.86963	0.68200	208	209	212	220	0	0	0	0	0.000
198	Si98	0.68706	0.82673	0.81933	150	209	210	218	0	0	0	0	0.000
199	O199	0.87260	0.05340	0.74420	187	188	0	0	0	0	0	0	0.000
200	O200	0.80840	0.05870	0.57890	188	189	0	0	0	0	0	0	0.000

201	O201	0.70070	0.05920	0.47110	189	190	0	0	0	0	0	0.000
202	O202	0.59690	0.06110	0.58560	190	191	0	0	0	0	0	0.000
203	O203	0.61490	0.05410	0.77630	191	192	0	0	0	0	0	0.000
204	O204	0.74350	0.05530	0.74600	188	192	0	0	0	0	0	0.000
205	O205	0.87420	0.84390	0.73720	193	194	0	0	0	0	0	0.000
206	O206	0.80850	0.84480	0.57280	194	195	0	0	0	0	0	0.000
207	O207	0.69800	0.84460	0.47120	195	196	0	0	0	0	0	0.000
208	O208	0.59100	0.83860	0.57770	196	197	0	0	0	0	0	0.000
209	O209	0.61690	0.84220	0.76940	197	198	0	0	0	0	0	0.000
210	O210	0.74480	0.84060	0.74220	194	198	0	0	0	0	0	0.000
211	O211	0.80470	0.94900	0.68660	0	194	0	0	0	0	0	0.000
212	O212	0.57680	0.94810	0.67690	0	197	0	0	0	0	0	0.000
213	O213	0.91610	0.12760	0.88960	162	187	0	0	0	0	0	0.000
214	O214	0.90860	-0.00170	0.91360	0	187	0	0	0	0	0	0.000
215	O215	0.90200	0.86860	0.92390	156	193	0	0	0	0	0	0.000
216	O216	0.68860	0.12980	0.88360	161	192	0	0	0	0	0	0.000
217	O217	0.69400	0.00070	0.90820	0	192	0	0	0	0	0	0.000
218	O218	0.69510	0.87090	0.91900	155	198	0	0	0	0	0	0.000
219	O219	0.49600	0.04250	0.70780	1	191	0	0	0	0	0	0.000
220	O220	0.49600	0.84720	0.70780	7	197	0	0	0	0	0	0.000
221	Si21	0.42238	0.44350	0.66402	147	233	247	248	0	0	0	0.000
222	Si22	0.30716	0.47228	0.81070	233	234	238	245	0	0	0	0.000
223	Si23	0.27911	0.43873	0.03120	0	235	285	286	0	0	0	0.000
224	Si24	0.12215	0.43702	0.02670	235	0	282	283	0	0	0	0.000
225	Si25	0.07128	0.47278	0.81449	236	237	246	0	0	0	0	0.000
226	Si26	0.18641	0.44104	0.67182	237	238	250	251	0	0	0	0.000
227	Si27	0.42265	0.67250	0.67282	35	148	239	249	0	0	0	0.000
228	Si28	0.30778	0.63016	0.81452	239	240	244	245	0	0	0	0.000
229	Si29	0.27554	0.67279	0.03109	37	0	241	284	0	0	0	0.000
230	Si30	0.12058	0.67310	0.02979	38	241	0	281	0	0	0	0.000
231	Si31	0.07044	0.63037	0.81800	242	243	246	0	0	0	0	0.000
232	Si32	0.18706	0.67327	0.68067	36	243	244	252	0	0	0	0.000
233	O233	0.37260	0.44660	0.75580	221	222	0	0	0	0	0	0.000
234	O234	0.30840	0.44130	0.92110	222	0	0	0	0	0	0	0.000
235	O235	0.20070	0.44080	0.02890	223	224	0	0	0	0	0	0.000
236	O236	0.09690	0.43890	0.91440	0	225	0	0	0	0	0	0.000
237	O237	0.11490	0.44590	0.72370	225	226	0	0	0	0	0	0.000
238	O238	0.24350	0.44470	0.75400	222	226	0	0	0	0	0	0.000
239	O239	0.37420	0.65610	0.76280	227	228	0	0	0	0	0	0.000
240	O240	0.30850	0.65520	0.92720	228	0	0	0	0	0	0	0.000
241	O241	0.19800	0.65540	0.02880	229	230	0	0	0	0	0	0.000

242	O242	0.09100	0.66140	0.92230	0	231	0	0	0	0	0	0	0.000
243	O243	0.11690	0.65780	0.73060	231	232	0	0	0	0	0	0	0.000
244	O244	0.24480	0.65940	0.75780	228	232	0	0	0	0	0	0	0.000
245	O245	0.30470	0.55100	0.81340	222	228	0	0	0	0	0	0	0.000
246	O246	0.07680	0.55190	0.82310	225	231	0	0	0	0	0	0	0.000
247	O247	0.41610	0.37240	0.61040	221	264	0	0	0	0	0	0	0.000
248	O248	0.40860	0.50170	0.58640	221	258	0	0	0	0	0	0	0.000
249	O249	0.40200	0.63140	0.57610	227	258	0	0	0	0	0	0	0.000
250	O250	0.18860	0.37020	0.61640	226	263	0	0	0	0	0	0	0.000
251	O251	0.19400	0.49930	0.59180	226	257	0	0	0	0	0	0	0.000
252	O252	0.19510	0.62910	0.58100	232	257	0	0	0	0	0	0	0.000
253	O253	0.99600	0.45750	0.79220	115	0	0	0	0	0	0	0	0.000
254	O254	0.99600	0.65280	0.79220	121	0	0	0	0	0	0	0	0.000
255	Si55	0.07762	0.55650	0.16402	109	267	281	282	0	0	0	0	0.000
256	Si56	0.19284	0.52772	0.31070	267	268	272	279	0	0	0	0	0.000
257	Si57	0.22089	0.56127	0.53120	251	252	268	269	0	0	0	0	0.000
258	Si58	0.37785	0.56298	0.52670	248	249	269	270	0	0	0	0	0.000
259	Si59	0.42872	0.52722	0.31449	270	271	280	287	0	0	0	0	0.000
260	Si60	0.31359	0.55896	0.17182	271	272	284	285	0	0	0	0	0.000
261	Si61	0.07735	0.32750	0.17282	73	110	273	283	0	0	0	0	0.000
262	Si62	0.19222	0.36984	0.31452	273	274	278	279	0	0	0	0	0.000
263	Si63	0.22446	0.32721	0.53109	75	250	274	275	0	0	0	0	0.000
264	Si64	0.37942	0.32690	0.52979	76	247	275	276	0	0	0	0	0.000
265	Si65	0.42956	0.36963	0.31800	276	277	280	288	0	0	0	0	0.000
266	Si66	0.31294	0.32673	0.18067	74	277	278	286	0	0	0	0	0.000
267	O267	0.12740	0.55340	0.25580	255	256	0	0	0	0	0	0	0.000
268	O268	0.19160	0.55870	0.42110	256	257	0	0	0	0	0	0	0.000
269	O269	0.29930	0.55920	0.52890	257	258	0	0	0	0	0	0	0.000
270	O270	0.40310	0.56110	0.41440	258	259	0	0	0	0	0	0	0.000
271	O271	0.38510	0.55410	0.22370	259	260	0	0	0	0	0	0	0.000
272	O272	0.25650	0.55530	0.25400	256	260	0	0	0	0	0	0	0.000
273	O273	0.12580	0.34390	0.26280	261	262	0	0	0	0	0	0	0.000
274	O274	0.19150	0.34480	0.42720	262	263	0	0	0	0	0	0	0.000
275	O275	0.30200	0.34460	0.52880	263	264	0	0	0	0	0	0	0.000
276	O276	0.40900	0.33860	0.42230	264	265	0	0	0	0	0	0	0.000
277	O277	0.38310	0.34220	0.23060	265	266	0	0	0	0	0	0	0.000
278	O278	0.25520	0.34060	0.25780	262	266	0	0	0	0	0	0	0.000
279	O279	0.19530	0.44900	0.31340	256	262	0	0	0	0	0	0	0.000
280	O280	0.42320	0.44810	0.32310	259	265	0	0	0	0	0	0	0.000
281	O281	0.08390	0.62760	0.11040	230	255	0	0	0	0	0	0	0.000
282	O282	0.09140	0.49830	0.08640	224	255	0	0	0	0	0	0	0.000

283	O283	0.09800	0.36860	0.07610	224	261	0	0	0	0	0	0	0.000
284	O284	0.31140	0.62980	0.11640	229	260	0	0	0	0	0	0	0.000
285	O285	0.30600	0.50070	0.09180	223	260	0	0	0	0	0	0	0.000
286	O286	0.30490	0.37090	0.08100	223	266	0	0	0	0	0	0	0.000
287	O287	0.50400	0.54250	0.29220	77	259	0	0	0	0	0	0	0.000
288	O288	0.50400	0.34720	0.29220	83	265	0	0	0	0	0	0	0.000

7 External Links

A voyage through “silicalite space” is found at

`http://www.vt4.tu-harburg.de/images/a/a8/Hexane_mfi_membrane_533K.mpeg`

The movie shows snapshots of 100 hexane molecules moving inside and on the surface of a silicalite membrane (red canyons and channels).

8 List of Symbols

Symbol	Description	Units
a	fitting parameter (chain-length influence on heat of adsorption)	kJ mol^{-1}
c	concentration (of labeled molecules)	mol m^{-3}
$\langle c_{\mathrm{gas}} \rangle$	mean concentration in gas phase	mol m^{-3}
c_i	concentration in slab number i	mol m^{-3}
Δc_i	incremental concentration change in slab number i	mol m^{-3}
$c_{i,\infty}$	concentration in slab number i after long time	
	(i.e. equilibrium concentration in that slab)	mol m^{-3}
c_i^*	normalized concentration in slab number i (i.e. $c_i/c_{i,\infty}$)	–
c_{labeled}	concentration of labeled molecules	mol m^{-3}
c_{surf}	concentration at membrane margin (i.e. at surface)	mol m^{-3}
$c_{\mathrm{surf},\infty}$	concentration at membrane margin after long time	
	(i.e. equilibrium surface concentration)	mol m^{-3}
c_{total}	concentration of labeled and unlabeled molecules	mol m^{-3}
$c_{\mathrm{unlabeled}}$	concentration of unlabeled molecules	mol m^{-3}
$\langle c_{\mathrm{zeol}} \rangle$	mean concentration in the adsorbed (zeolite) phase	
	(i.e. equilibrium concentration)	mol m^{-3}
D	diffusion coefficient	m^2 s^{-1}
D_{S}	self-diffusion coefficient	m^2 s^{-1}
$D_{\mathrm{S,eff}}$	effective self-diffusion coefficient	m^2 s^{-1}
$D_{\mathrm{S}}^{\mathrm{dcTST}}$	self-diffusion coefficient from dynamically corrected	
	transition state theory	m^2 s^{-1}
F	free energy	J
$\Delta\beta F^{\ddagger}$	normalized difference between free energy at surface barrier and	
	at diffusion barrier [i.e. $\beta(F_{\mathrm{surf}}^{\ddagger} - F_{\mathrm{zeol}}^{\ddagger})$]	–
F_{gas}	free energy in gas phase	J

Symbol	Description	Units
$F^{\ddagger}_{\mathrm{surf}}$	free energy at surface barrier	J
F_{zeol}	free energy at intracrystalline well	J
ΔF_{zeol}	free-energy barrier of elementary intracrystalline diffusion event	J
$F^{\ddagger}_{\mathrm{zeol}}$	free energy at intracrystalline diffusion barrier	J
ΔH_{ads}	isosteric heat of adsorption	kJ mol^{-1}
$\Delta H_{\mathrm{ads},0}$	fitting parameter (chain-length influence on heat of adsorption)	kJ mol^{-1}
j	equilibrium molar flux	mol m^{-2} s^{-1}
$j^{\ddagger}_{\mathrm{dcTST}}$	equilibrium molar flux at location of barrier on the basis of dynamically corrected transition state theory (i.e. with κ)	mol m^{-2} s^{-1}
j_{gas}	equilibrium molar flux in gas phase	mol m^{-2} s^{-1}
$j^{\ddagger}_{\mathrm{surf}}$	equilibrium molar flux at location of surface barrier	mol m^{-2} s^{-1}
$j^{\ddagger}_{\mathrm{zeol}}$	equilibrium molar flux at location of intracrystalline diffusion barrier	mol m^{-2} s^{-1}
$j^{\ddagger}_{\mathrm{TST}}$	equilibrium molar flux at location of barrier on the basis of transition state theory (i.e. without κ)	mol m^{-2} s^{-1}
k_{bend}	energy constant of bond-angle bending potential	J, J rad^{-2}
k_{bond}	energy constant of harmonic bond vibration potential	J Å^{-2}
k_i	energy constant of potential type i	J, J Å^{-2}, J rad^{-2}
k_{B}	Boltzmann constant ($1.3806488{\cdot}10^{-23}$)	J K^{-1}
K_{H}	Henry coefficient	–
L	dimensionless ratio of permeability to diffusivity [i.e. $(\delta/2)\alpha/D_{\mathrm{S}}$]	–
m_{fluid}	mass of atom/bead	kg
M	tracer mass adsorbed	kg
M_{∞}	tracer mass adsorbed after long time (i.e. adsorption capacity)	kg
n	number of CH_x beads in molecule (chain length)	–
n_{s}	number of slabs along q	–

Symbol	Description	Units
p	pressure	Pa
p^*	reduced pressure (i.e. p/p_{crit})	–
p_{crit}	critical pressure	Pa
P	residence probability	–
$P^{\ddagger}_{\mathrm{surf}}$	residence probability at surface barrier [i.e. $P(q^{\ddagger}_{\mathrm{surf}})$]	–
P_{zeol}	residence probability at intracrystalline free-energy well [i.e. $P(q_{\mathrm{zeol}})$]	–
$P^{\ddagger}_{\mathrm{zeol}}$	residence probability at intracrystalline diffusion barrier [i.e. $P(q^{\ddagger}_{\mathrm{zeol}})$]	–
q	reaction coordinate	Å
$q^{\ddagger}$	location of barrier	Å
$q^{\ddagger}_{\mathrm{surf}}$	location of surface barrier	Å
$q^{\ddagger}_{\mathrm{surf,l}}$	location of surface barrier at left membrane side	Å
$q^{\ddagger}_{\mathrm{surf,r}}$	location of surface barrier at right membrane side	Å
q_{zeol}	location of intracrystalline free-energy well	Å
$q^{\ddagger}_{\mathrm{zeol}}$	location of intracrystalline diffusion barrier	Å
q_{A}	location of free-energy well on barrier's left	Å
q_{B}	location of free-energy well on barrier's right	Å
r	atomic distance	Å
r_{eq}	atomic equilibrium distance	Å
r_{pore}	radius from pore center	Å
R	universal gas constant (8.314)	J mol^{-1} K^{-1}
t	time	s
Δt	time increment of tracer-exchange simulation	s
T	temperature	K
T^*	reduced temperature (i.e. T/T_{crit})	–

Symbol	Description	Units
T_{crit}	critical temperature	K
T_{ref}	reference temperature (i.e. $1.05 \cdot T_{\mathrm{crit}}$)	K
U	potential energy	J
U_{bend}	intramolecular potential energy due to bond-angle bending	J
U_{bond}	intramolecular potential energy due to bond vibration	J
U_{torsion}	intramolecular potential energy due to dihedral-angle twist	J
x	Cartesian coordinate	m
X	dimensionless coefficient	
	{i.e. $\exp[(a \cdot n + \Delta H_{\mathrm{ads},0})/R \cdot (1/T - 1/T_{\mathrm{ref}})]$}	–
y	Cartesian coordinate	m
y_{UC}	size of unit cell in y direction	Å
z	Cartesian coordinate	m
Δz	spatial grid fineness of tracer-exchange simulation	m
z_i	position of slab number i	m
z_{UC}	size of unit cell in z direction	Å
α	surface permeability	$\mathrm{m\,s^{-1}}$
β	$= 1/(k_{\mathrm{B}}T)$	$\mathrm{J^{-1}}$
β_{ref}	$= 1/(k_{\mathrm{B}}T_{\mathrm{ref}})$	$\mathrm{J^{-1}}$
γ_i	i-th positive root of $\gamma_i \tan \gamma_i = L$	–
δ	membrane thickness	m
δ_{crit}	critical membrane thickness	m
	atom/bead types i and j	J

Symbol	Description	Units
ε	Lennard-Jones interaction parameter (energy)	J
ε_{ij}	Lennard-Jones energy parameter between	
$\Delta\varepsilon$	relative difference between Lennard-Jones energy	
	parameters	–
η_i	i-th parameter of torsion potential	J
θ	unit-cell loading	molecules (unit cell)$^{-1}$
κ	transmission coefficient	–
κ_{surf}	transmission coefficient of hop at membrane surface	–
$\kappa_{\mathrm{surf,l}}$	transmission coefficient of hop at left membrane surface	–
$\kappa_{\mathrm{surf.r}}$	transmission coefficient of hop at right membrane surface	–
κ_{zeol}	transmission coefficient of elementary intracrystalline	
	diffusion event	–
λ	hop distance of an elementary diffusion event	m, Å
π	3.141592653589793238	–
σ	Lennard-Jones interaction parameter (size)	Å
σ_{ij}	Lennard-Jones size parameter between	
	atom/bead types i and j	Å
$\sigma_{\mathrm{original}}$	original Lennard-Jones size parameter	Å
$\Delta\sigma$	relative difference between Lennard-Jones size	
	parameters [i.e. $\Delta\sigma = (\sigma - \sigma_{\mathrm{original}})/\sigma_{\mathrm{original}}$]	–
ϕ	angle (bond angle and dihedral angle)	$^\circ$
ϕ_{eq}	equilibrium angle (bond angle and dihedral angle)	$^\circ$

References

(1) Zimmermann, N. E. R.; Smit, B.; Keil, F. J. *J. Phys. Chem. C* **2010**, *114*, 300–310.

(2) Dubbeldam, D.; Beerdsen, E.; Vlugt, T. J. H.; Smit, B. *J. Chem. Phys.* **2005**, *112*, 224712.

(3) Dubbeldam, D.; Calero, S.; Vlugt, T. J. H.; Krishna, R.; Maesen, T. L. M.; Smit, B. *J. Phys. Chem. B* **2004**, *108*, 12301–12313.

(4) Liu, B.; Smit, B.; Rey, F.; Valencia, S.; Calero, S. *J. Phys. Chem. C* **2008**, *112*, 2492–2498.

(5) Heinke, L.; Kärger, J. *Phys. Rev. Lett.* **2011**, *106*, 074501.

(6) Jakobtorweihen, S.; Hansen, N.; Keil, F. J. *Mol. Phys.* **2005**, *103*, 471–489.

(7) Zimmermann, N. E. R.; Haranczyk, M.; Sharma, M.; Liu, B.; Smit, B.; Keil, F. J. *Mol. Simul.* **2011**, *37*, 986–989.